

# Numerical study on mixed convection flow of heat source modules mounted on a horizontal plate

Abhishek Anand

A Thesis Submitted to  
Indian Institute of Technology Hyderabad  
In Partial Fulfillment of the Requirements for  
The Degree of Master of Technology



भारतीय प्रौद्योगिकी संस्थान हैदराबाद  
Indian Institute of Technology Hyderabad

Department of Mechanical Engineering

August 2011

# Declaration

I declare that this written submission represents my ideas in my own words, and where ideas or words of others have been included, I have adequately cited and referenced the original sources. I also declare that I have adhered to all principles of academic honesty and integrity and have not misrepresented or fabricated or falsified any idea/data/fact/source in my submission. I understand that any violation of the above will be cause for disciplinary action by the Institute and can also evoke penal action from the sources that have thus not been properly cited, or from whom proper permission has not been taken when needed.

---

(Signature)

---

Abhishek Anand

Student Name

---

ME09G001

Roll No

## Approval Sheet

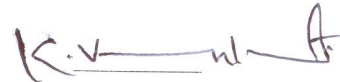
This thesis titled 'Numerical study on mixed convection flow of heat source modules mounted on a horizontal plate' by Mr. Abhishek Anand is approved for the degree of Master of Technology.



Examiner  
(Dr. Raja Banerjee)



Examiner  
(Dr. Vinod)



Adviser  
(Dr. K. Venkatasubbaiah)



Chairman  
(Dr. Narasimhamangal)

# Acknowledgements

I would like to express my profound respect for my supervisor Dr. K. Venkatasubbaiah. He is the person who has sculpted me to my current shape and has shown me the right direction to discover myself. The little work that I have done has been possible only because of his excellent guidance. Like a parent, he always kept a watchful eye on our personal needs and problems. During the two years of my M.Tech work, I never felt away from home owing to his parent-like company. I can say right from the deep of my heart that the guidance, I have received from him, is unprecedented. I am grateful to him for the valuable suggestions and inputs that he have provided from time to time.

I am extremely thankful to the Monks of Ramkrishna Mission, Pankaj Maharaj, Anumpamanadaji Maharaj, who always lovingly helped me to correct my self and right advice whenever I needed. I am also very lucky that during my stay at my I.I.T Madras, I came in contact of volunteer of VSC (Vivekanada Study Circle). The experience that helped me to have a broader out look of life and many experience. I would like to mention the name of Rahul Jee, Mauraya, K. Vishwanath and other volunteers who gave a long lasting friends which makes me aware of the various other avenues of life and our country. I am really thankful to my friends Minesh, Prasant Patel, Bhanu Kumar Masna, Bhagat, Soma Shekara M A, Balan, Chandrakant Kumar Nirala, Meenakshi Devi Pare, Srinivas Goud, Ummaiya, Santosh, C S Arun and juniors of 1st year M.Tech (Now in 2nd year) for there nice company. Being with them is a nice experience that will be in the album of my memory for my entire life. Coming to my family I am will remember to

My special thanks to Teja without whom it was not possible to complete this thesis report.

It is the time to take the name of my better half Animesh Anand. I am truly indebted

to her for his inspiration, patience and sacrifices. His company helped me to overcome many difficult situations. His inspiration used to work like a tonic to revive my determination and self-confidence after any failure. Above all, he is a person who, I believe, has brought good fortune for me.

**Abhishek Anand**



*To*  
*My Loving Parents*





# Abstract

Mixed convection flow of heat source modules mounted on a horizontal plate has been studied numerically. Present analysis is valid when the buoyancy force effects are small compared to forced convection effects. The mixed convection flow problem is formulated by two-dimensional incompressible flow with the buoyancy term represented by Boussinesq approximation. The governing equations are transformed into an orthogonal transformed plane and solved in stream function and vorticity formulation using high accuracy finite difference schemes. Results are reported for single and double heat sources mounted on horizontal plate with and without thickness of the heat source module. Detailed results are reported on the thermal field of heat source modules or electronic components mounted on a horizontal plate and its dependence on physical parameters such as the external velocity, energy input, thickness and location of heat source modules etc. Results show that the surface temperature decreases with the increase of free stream velocity. The surface temperature decreases with the increase of energy input to the heat source due to buoyancy. The location of the heat source shows significant effect on the surface temperature and thermal field near the heat source. The surface temperature increases with the increase of heat source location from the leading edge of the plate due to increase of thermal boundary layer thickness. The distance between the two heat sources shows a significant effect on thermal field near the heat source modules. The surface temperature decreases with the increase of thickness of the heat source module due to increase of surface area. The maximum surface temperature and average Nusselt number values are reported for various combinations of Reynolds and Richardson numbers. The reported average Nusselt numbers are matching very well with the experimental results available from the literature.

## Nomenclature

$T_\infty$	Free stream temperature
$U_\infty$	Free stream velocity
$T_s$	Surface Temperature
$u$ and $v$	velocities in the x and y directions
$\beta_t$	volumetric thermal expansion coefficient
$k$	thermal conductivity of the fluid
$c_p$	specific heat of fluid
$\nu$	Kinematic Viscosity
$\alpha$	Thermal diffusivity
$g$	acceleration due to gravity
$q$	Constant Heat flux
$L$	Width of the heat source module
$H$	Thickness of the heat source module
$\theta$	Nondimensional temperature
$U^*$	Dimensionless velocity
$Gr$	Grashof number
$Re$	Reynolds number
$Ri$	Richardson number
$\psi$	Stream function
$\omega$	Vorticity
$Pr$	Prandtl number
$h_1$ and $h_2$	Scale factors
$h$	Convective heat transfer coefficient
$Nu_l$	Local Nusselt Number
$Nu_{avg}$	Average Nusselt Number

# Contents

<b>Abstract</b>	<b>i</b>
<b>List of Figures</b>	<b>vii</b>
<b>List of Tables</b>	<b>ix</b>
<b>Nomenclature</b>	<b>x</b>
<b>1 Introduction</b>	<b>1</b>
1.1 Motivation . . . . .	1
1.2 Problem Statement . . . . .	2
1.3 Literature Survey . . . . .	2
1.4 Objectives of present study . . . . .	3
1.5 Overview of thesis . . . . .	4
<b>2 Governing equations and Boundary conditions</b>	<b>27</b>
2.1 Boussinesq Approximation . . . . .	28
2.1.1 Conservation of mass . . . . .	28
2.1.2 Conservation of momentum . . . . .	29
2.1.3 Conservation of energy . . . . .	30
2.2 Boundary condition . . . . .	30
2.3 Non-dimensionlization of governing equations . . . . .	31
2.3.1 Non Dimensionised Equation . . . . .	31
2.3.2 Non Dimensionlization of Boundary Condition . . . . .	32
2.4 stream function and vorticity formulation: . . . . .	33

2.4.1	Stream Function . . . . .	33
2.4.2	Vorticity . . . . .	34
2.5	Vorticity transport equation . . . . .	34
2.6	Orthogonal Transformation From x-y domain to $\xi - \eta$ domain . . . . .	34
2.7	Transformation of the Boundary Conditions From Physical Plane to the Computational Plane . . . . .	36
2.8	Nusselt Number . . . . .	37
<b>3</b>	<b>Numerical Methods</b>	<b>38</b>
<b>4</b>	<b>Flush mounted heat source modules results</b>	<b>40</b>
4.1	Single flush heat source module . . . . .	40
4.2	Double flush heat source modules . . . . .	49
<b>5</b>	<b>Heat source modules with thickness</b>	<b>54</b>
5.1	Single heat source module with thickness . . . . .	54
5.2	Double heat source modules with thickness . . . . .	66
<b>6</b>	<b>Conclusion</b>	<b>77</b>
	<b>Bibliography</b>	<b>79</b>

# List of Figures

2.1	Flow field and coordinate system . . . . .	27
4.1	Temperature contours with different grid points . . . . .	41
4.2	Stream Function contours with different grid points . . . . .	41
4.3	Vorticity contours with different grid points . . . . .	42
4.4	Temperature contours with different times for $Re = 350$ and $Ri = 0.0$ . . .	42
4.5	Stream Function Contours with different time for $Re = 350$ and $Ri = 0.0$ .	43
4.6	Vorticity Contours with different time for $Re = 350$ and $Ri = 0.0$ . . . . .	43
4.7	Surface Temperature with at $t = 5, 10, 15$ and $20$ for $Re = 350$ and $Ri = 0$	44
4.8	Surface temperature contour different Reynolds Number for $Ri = 0$ and Loc = 2 - 3 . . . . .	44
4.9	Surface temperature with different Reynolds Number for $Ri = 0$ and Loc = 3 - 4 . . . . .	45
4.10	Temperature contours with different times for $Re = 350$ and $Ri = 0.1$ . . .	45
4.11	Stream function contours with different times for $Re = 350$ and $Ri = 0.1$ .	46
4.12	Vorticity contours with different times for $Re = 350$ and $Ri = 0.1$ . . . . .	46
4.13	Surface temperature with different Richardson number for $Re = 350$ . . . .	47
4.14	Surface temperature with different Flush source location for $Ri = 0.0$ . . .	48
4.15	Surface temperature with different Flush source location for $Ro = 0.1$ . . .	48
4.16	Nondimensionlazier Temperature contours in flow field for different time .	50
4.17	Vorticity contours in flow field for different time . . . . .	50
4.18	Stream Function in flow field for different time . . . . .	51
4.19	Surface temperature for different Re for, $Ri = 0.1$ at $t=20$ . . . . .	51

4.20	Surface temperature for different Re for, $Ri = 0.1$ at $t=20$ . . . . .	52
4.21	Surface temperature for different heat source location for, $Ri = 0.1$ at $t=20$	52
5.1	Temperature contours at $t = 5, 10, 15$ and $20$ . . . . .	54
5.2	Zoomed view of Temperature contours near heat source modules at $t = 5,$ $10, 15$ and $20$ . . . . .	55
5.3	Vorticity contours at $t = 5, 10, 15$ and $20$ . . . . .	56
5.4	Stream function contours at $t = 5, 10, 15$ and $20$ . . . . .	56
5.5	Surface temperature at $t = 5, 10, 15$ and $20$ . . . . .	57
5.6	Effect of Richardson number on Surface temperature for $Re = 350$ and $H/L$ $= 0.25$ . . . . .	57
5.7	Effect of Richardson number on Vorticity contours for $Re = 350$ and $H/L$ $= 0.25$ . . . . .	58
5.8	Effect of Reynolds number on surface temperature for $Ri = 0.1$ and $H/L$ $= 0.25$ . . . . .	58
5.9	Effect of Reynolds number on temperature contours for $Ri = 0.1$ and $H/L$ $= 0.25$ . . . . .	59
5.10	Effect of Reynolds number on temperature contours for $Ri = 0.1$ and $H/L$ $= 0.25$ . . . . .	60
5.11	Effect of Reynolds number on vorticity contours for $Re = 435$ and $835$ . .	60
5.12	Effect of Reynolds number on vorticity contours for $Re = 350$ and $835$ . .	61
5.13	Effect of location on heat source module on surface temperature for $H/L$ $= 0.25$ and $Re = 350$ . . . . .	62
5.14	Effect of location on heat source module on surface temperature for $H/L$ $= 0.50$ and $Re = 350$ . . . . .	62
5.15	Effect of location on heat source module on vorticity contours for $H/L =$ $0.25$ and $Re = 350$ . . . . .	63
5.16	Effect of location on heat source module on vorticity contours for $H/L =$ $0.50$ and $Re = 350$ . . . . .	63
5.17	Effect of thickness on heat source module on surface temperature for $Ri =$ $0.1$ and $Re = 350$ . . . . .	64

5.18	Effect of thickness on heat source module on Vorticity contours for $Ri = 0$ and $Re = 350$ . . . . .	65
5.19	Effect of thickness on heat source module on surface temperature for $Ri =$ $0.1$ and $Re = 350$ . . . . .	65
5.20	Surface temperature at $t = 5, 10, 15,$ and $20$ . . . . .	67
5.21	Stream function contours at $t = 5, 10, 15$ and $20$ . . . . .	67
5.22	Vorticity contours at $t = 5, 10, 15$ and $20$ . . . . .	68
5.23	Temperature contours at $t = 5, 10, 15$ and $20$ . . . . .	68
5.24	Effect of heat module thickness on surface temperature for $Ri = 0$ . . . .	69
5.25	Effect of heat module thickness on surface temperature for $Ri = 0.1$ . . . .	69
5.26	Effect of space between heat source module on surface temperature for $Ri$ $= 0.1$ . . . . .	70
5.27	Effect of space between heat source module on surface temperature for $Ri$ $= 0$ . . . . .	71
5.28	Effect of spacing of heat source module on Vorticity contours for $Ri = 0$ . .	71
5.29	Effect of spacing of heat source module on Vorticity contours for $Ri = 0.1$ .	72
5.30	Effect of Reynolds Number on surface temperature of the plate . . . . .	72
5.31	Effect of Reynolds Number on surface temperature of the plate . . . . .	73
5.32	Effect of Reynolds Number on vorticity contours in flow field for $H/L = 0.5$	74
5.33	Effect of Reynolds Number on vorticity contours in flow field for $H/L = 0.25$	74





# List of Tables

4.1	Average Nusselt number and maximum surface temperature with different grid points for $Re = 350$ , $Ri = 0.1$ . . . . .	40
4.2	Maximum surface temperature and average Nusselt number values for flush source modules . . . . .	49
4.3	Maximum surface temperature and average Nusselt number values for two flush heat source modules . . . . .	53
5.1	Plate with single heat source modules . . . . .	66
5.2	Average Nusselt number and maximum surface temperature for the double heat source modules . . . . .	75



# Chapter 1

## Introduction

### 1.1 Motivation

Mixed convection flows, resulting from simultaneous buoyancy and forced convection effects, arises in environmental and electronics cooling processes. In studying forced convective heat transfer flow over a horizontal surface, it is customary to neglect the effect of buoyancy forces. Such approach may not be justified because the buoyancy force arises when the velocity is small and the temperature difference between the surface and ambient is large. The buoyancy force induces a longitudinal pressure gradient which in turn alters the flow field and heat transfer rate from the surface.

The effect of incorporation of both forced and natural convection mechanisms on the heat transfer rate is particularly important in the design of thermal systems for electronics cooling. One of the major constraint of the better design and efficient working of the major electronic devices are decided by the maximum temperature attained by the device. High computation speeds for modern applications are possible only by increasing the integrated circuit densities. The development of such applications will, however, place extraordinary demand on thermal design. So it is important to investigate the thermal field of heat source modules or electronic components mounted on a horizontal plate and its dependence on physical parameters such as the external velocity, energy input, thickness and location of heat source modules etc.

Present study has been motivated due to the following reasons

- Detailed numerical study does not exist in the literature for the mixed convection flow from heat source modules mounted on a horizontal plate.
- Accurate results do not exist to predict maximum surface temperature on the heat source module with varying physical parameters.

## 1.2 Problem Statement

Numerical study on mixed convection flow of heat source modules mounted on a horizontal plate

- Effects of external free stream velocity and energy input to the heat source
- Effects of heat source parameters like location ,thickness, single and multiple heat sources

## 1.3 Literature Survey

External induced flow cooling system must be employed in high power dissipating electronic systems. The chip industry is far developed than ever before. To reduce the size of equipment or to increase more chips to be packed in smaller area miniature chips are being used. These give the more thermal energy out because of the reduced size. The use of chips acts as miniature heat source and it keeps emitting the heat. The proper working of the electric appliances mainly depends on the maximum temperature attained by the device. The heat generated by these chips to be removed quickly else degrades the performance of the sensitive appliances. Maximum heat removal from the electronic system gives more efficiency and long life of the system. More details of chip cooling are given in Kraus *et.al* [1]

In the literature, Kang and Jaluria[2] have studied the natural convection heat transfer characteristics from protruding thermal source located on horizontal and vertical surfaces. They found that a freely rising plume was generated by the heat source when it is located on a horizontal surface. Fuji et al.[3] studied numerically and experimentally for the

natural convection from an array of vertical parallel plates with discrete and protruding heat sources. Afraid and Zebib [4] have studied numerically for natural convection cooling of heated components mounted on a vertical wall. Park and Bergles [5] have studied experimentally for natural convection heat transfer characteristics of simulated microelectronic chips mounted on a vertical wall. It was found that the heat transfer coefficient increases with increasing width. Even though natural convection cooling is still used in small systems, an externally induced flow must be employed in high power dissipating systems. Incropera [6] studied experimentally for forced convection from heat sources mounted flush on the bottom surface of a horizontal channel. Zebib and Wo [7] have studied forced air cooling in a constricted channel using finite difference methods. Devalath and Bayazitoglu [8] have studied forced convective cooling of multiple rectangular blocks with uniform heat flux. Kennedy and Zebib [9] have studied numerically and experimentally the effect of buoyancy in a laminar horizontal channel flow with an isolated heat source on the lower or upper wall. Jaluria [10] studied mixed convection flow over localized multiple thermal sources mounted on a vertical surface. He considered that heat source was mounted flush on the surface means with negligible thickness. Kang et al.[11] studied experimentally for mixed convection flow from an isolated heat source module on a horizontal plate. They have reported that location of maximum temperature on the module surface which corresponds to the minimum local convective heat transfer coefficient. They have also reported that module thickness influences on the heat transport. A comprehensive review of mixed convection flows were given in Gebhart et al. [12]. Recently, Venkatasubbaiah[13] studied the effect of buoyancy on the stability mixed convection flow over a horizontal plate. He reported that buoyancy has significant effect on heat transfer rate.

## 1.4 Objectives of present study

In the present study our aim is to find thermal field near the heat sources

- To develop accurate numerical method to estimate maximum temperature of heat sources.

- To study the effect of free stream velocity and energy input of the heat sources.
- To study the effect of heat source location and thickness.
- To study the effect of single and multiple heat sources.

## **1.5 Overview of thesis**

- Chapter 2 deals with the governing equations of two dimensional incompressible mixed convection flows over heat source modules mounted on horizontal plate with boundary and initial conditions. Stream function and vorticity formulation is given.
- Chapter 3 deals the numerical methods.
- Chapter 4 discusses the results for single and multiple flush heat sources.
- Chapter 5 discusses the results for single and multiple heat sources with thickness.
- Chapter 6 discusses the summary and conclusions of the present study.
- Figures and tables are placed where they were cited first.

# Chapter 2

## Governing equations and Boundary conditions

Consider the laminar two-dimensional motion of fluid past heat source modules mounted on a horizontal plate, with the free stream velocity and temperature denoted by,  $U_\infty$  and  $T_\infty$ . The schematic diagram and the co-ordinate system is show in Fig. 2.1. The surface and heat source modules are taken as wide in the transverse direction so that a two-dimensional flow is obtained. The leading edge of the plate is considered as the stagnation point. Heat source of height  $H$  and width  $L$  is located on a horizontal plate at distance  $L_1$  from leading edge and  $L_2$  from trailing edge. The heat source is emitting heat with constant flux  $q$ . We have considered two cases of single and multiple flush heat sources and heat sources with thickness.

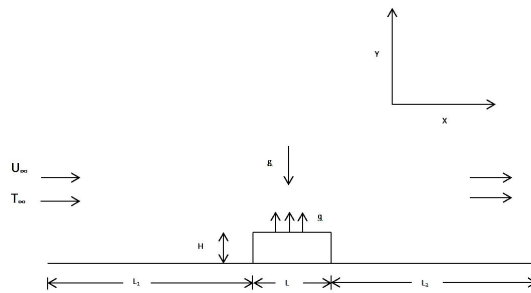


Figure 2.1: Flow field and coordinate system

## 2.1 Boussinesq Approximation

The buoyancy forces that arise as a result of temperature differences and that cause fluid flow in free convection, also exist in forced convection flow. For low speed flows, the density changes associated to temperature changes are at most 1 percent. So we may treat the density as a constant in all terms of the governing equations except in the buoyancy force term. This is the well-known Boussinesq approximation.

As the density variation is only due to temperature variation we can use a variable  $\beta_t$ , volumetric thermal expansion coefficient

$$\beta_t = -\frac{1}{\rho} \left( \frac{\partial \rho}{\partial T} \right)_p \quad (2.1)$$

$\beta_t$ , measures the change in the density of the fluid in response to change in the temperature. In mathematical form it can be written as,

$$\beta_t \approx -\frac{1}{\rho} \left( \frac{\partial \rho}{\partial T} \right)_p = -\frac{1}{\rho} \frac{\rho_\infty - \rho}{T_\infty - T} \quad (2.2)$$

it can be written as

$$(\rho_\infty - \rho) \approx \rho \beta_t (T - T_\infty) \quad (2.3)$$

All fluid properties are assumed to be constant, except that the density variations within the fluid are considered only to the extent that they contribute to the buoyancy forces. Governing equations are the incompressible continuity, momentum and energy equations with fluid flow properties taken as constant and buoyancy force term modeled with Boussinesq approximation.

### 2.1.1 Conservation of mass

The conservation of mass means, this equation comes from the principle of conservation of mass, i.e mass can neither be created nor destroyed .It is obtained by taking the mass



balance in the control volume equating the amount of fluid entering and leaving.

$$\frac{\partial u}{\partial x} + \frac{\partial v}{\partial y} = 0 \quad (2.4)$$

## 2.1.2 Conservation of momentum

The momentum equation is derived from the Newton's second law of motion. The amount of external force acting is equal to the rate of change of momentum. There are two types of forces are acting on the body.

- Body forces

The forces are proportional to the volume of the body. Gravitational force , buoyancy force .These forces can be resolved in the x and y direction .

- Surface forces

The forces proportional to the surface area of the body. The surface forces are due to the static pressure and viscous stress. While the static force is always normal to surface the viscous force can be resolved into two perpendicular component normal stress and shear stress.

The normal stress always produces the linear deformation while the shear force always produces the angular deformation.

The Navier Stokes equation for the steady, two dimensional flow of an incompressible fluid with constant properties ( except the change in the density due to temperature variation ) in the x direction can be written as

$$\frac{\partial u}{\partial t} + u \frac{\partial u}{\partial x} + v \frac{\partial u}{\partial y} = -\frac{1}{\rho} \frac{\partial p}{\partial x} + \frac{\mu}{\rho} \left( \frac{\partial^2 u}{\partial x^2} + \frac{\partial^2 u}{\partial y^2} \right) \quad (2.5)$$

The left hand terms of the equation shows the rate of the momentum transfer from the control volume in the x direction. In equation (2.9) Right hand terms  $-\frac{1}{\rho} \frac{\partial p}{\partial x}$  shows the net pressure force acting in the x direction.

The second term represents the net effect of the viscous normal and shear stress.

$$\frac{\partial v}{\partial t} + u \frac{\partial v}{\partial x} + v \frac{\partial v}{\partial y} = -\frac{1}{\rho} \frac{\partial p}{\partial y} + g\beta_t(T - T_\infty) + \frac{\mu}{\rho} \left( \frac{\partial^2 u}{\partial x^2} + \frac{\partial^2 u}{\partial y^2} \right) \quad (2.6)$$

Where,  $g$ , acceleration due to gravity:  $\beta_t$  is a fluid property called volumetric thermal expansion coefficient:  $\mu$  and  $\rho$  are the dynamic viscosity and density of the fluid.

### 2.1.3 Conservation of energy

The conservation of energy equation written in differential form neglecting the heat generation as

$$\frac{\partial T}{\partial t} + u \frac{\partial T}{\partial x} + v \frac{\partial T}{\partial y} = \frac{k}{\rho c_p} \left( \frac{\partial^2 T}{\partial x^2} + \frac{\partial^2 T}{\partial y^2} \right) \quad (2.7)$$

The conservation of the energy is obtained from the conservation of energy in a differential control volume. In the left hand side first term shows the unsteady state condition; second and third terms shows the convective terms. Right hand side terms shows the diffusion (conduction ) phenomena.

where  $k$  is thermal conductivity of the fluid;  $c_p$  is specific heat of fluid

## 2.2 Boundary condition

The schematic diagram of heat source module as shown in Fig. 2.1

No slip boundary conditions at the surface for velocity field and constant heat flux on the heat source and rest of the plate is adiabatic conditions for temperature field. At the inlet and top of the domain considered as free stream boundary conditions. At the outlet the velocity and temperature fields considered as fully developed conditions.

The imposed boundary condition is

- At the wall surface

$$v = u = 0$$

$$\frac{\partial T}{\partial y} = 0 \text{ for } 0 \leq x \leq L_1 \text{ at } y = 0$$

$$\frac{\partial T}{\partial y} = -\frac{q}{k} \text{ for } L_1 \leq x \leq L_1 + L \text{ at } y = h$$

$$\frac{\partial T}{\partial y} = 0 \text{ for } L_1 + L \leq x \leq L_1 + L + L_2 \text{ at } y = 0$$

- At inlet and at top

$$u = U_\infty; v = 0; T = T_\infty$$

- At out let

$$\frac{\partial T}{\partial x} = 0; \frac{\partial v}{\partial y} = 0$$

The initial condition,  $t = 0$  is considered as inviscid solution over the flat plate.

## 2.3 Non-dimensionlization of governing equations

In general two or more physical properties are associated with the equation which are not completely independent. Nondimensionaslationsing makes the equation simpler and give some important non dimensionisation numbers. These non dimesionationlized number gives the independence to perform fewer simulation that gives the infinite combination of physically important parameters.

Non dimensionlisation of the equation has been done by using the appropriate Length , velocity, temperature ,and pressure scales.

The equation are nondimensionalized by using the following variables.

$$X^* = \frac{x}{L}; Y^* = \frac{y}{L}; U^* = \frac{u}{U_\infty}; V^* = \frac{v}{U_\infty}; t^* = \frac{t}{\frac{L}{U_\infty}}; \theta = \frac{T - T_\infty}{\frac{q(L+2H)}{k}}; P^* = \frac{P - P_\infty}{\rho U_\infty^2}$$

### 2.3.1 Non Dimensionised Equation

After substituting the above variables in the governing equations (2.13) to (2.16) for velocity and temperature fields as given by,

$$\frac{\partial U^*}{\partial X^*} + \frac{\partial V^*}{\partial Y^*} = 0 \quad (2.8)$$

$$\frac{\partial U^*}{\partial t^*} + U^* \frac{\partial U^*}{\partial X^*} + V^* \frac{\partial U^*}{\partial Y^*} = \frac{1}{Re} \left( \frac{\partial^2 U^*}{\partial X^{*2}} + \frac{\partial^2 U^*}{\partial Y^{*2}} \right) - \frac{\partial P}{\partial X^*} \quad (2.9)$$

$$\frac{\partial V^*}{\partial t^*} + U^* \frac{\partial V^*}{\partial X^*} + V^* \frac{\partial V^*}{\partial Y^*} = \frac{1}{Re} \left( \frac{\partial^2 V^*}{\partial X^{*2}} + \frac{\partial^2 V^*}{\partial Y^{*2}} \right) - \frac{\partial P}{\partial Y^*} + \frac{Gr\theta}{Re^2} \quad (2.10)$$

$$\frac{\partial \theta}{\partial t^*} + U^* \frac{\partial \theta}{\partial X^*} + V^* \frac{\partial \theta}{\partial Y^*} = \frac{1}{RePr} \left( \frac{\partial^2 \theta}{\partial X^{*2}} + \frac{\partial^2 \theta}{\partial Y^{*2}} \right) \quad (2.11)$$

where  $Gr = \frac{g\beta_t q(L+2H)L^3}{K\nu^2}$  is the Grashof number. Grashof number is important for natural convection. It indicates the ratio of the Buoyancy force to viscous force. ;  $Re = \frac{U_\infty L}{\nu}$  is Reynolds number. Reynolds Number is important for the forced convection, it gives the ratio of the inertia force to viscous force.

$Pr = \frac{\nu}{\alpha}$  is a Prantal number which gives the ratio of momentum diffusivity and thermal diffusivity.;  $g$  is the gravitational force per unit mass;  $\alpha$  and  $\nu$  are thermal diffusivity and kinematic viscosity.

$Ri = \frac{Gr}{Re^2}$  is the Richardson number (Ri). The Richardson number provides a measure of the infulence of free convection in comprasions with forced convection. When  $Ri = \frac{Gr}{Re^2} \approx 1$  it is a mixed convection flow.

### 2.3.2 Non Dimensionlization of Boundary Condition

- Inlet and top of flow domain

$$V^* = 0; \quad U^* = 1; \quad \Theta = 0;$$

- Out Flow Condition

$$\frac{\partial \Theta}{\partial X^*} = 0; \quad \frac{\partial V^*}{\partial X^*} = 0$$

- Wall Boundary Condition

$$V^* = U^* = 0$$

$$\frac{\partial \Theta}{\partial Y^*} = 0 \quad for \quad 0 < X^* < \frac{L_1}{L} \quad At \quad Y^* = 0$$

$$\frac{\partial \Theta}{\partial Y^*} = -1 \quad for \quad \frac{L_1}{L} < X^* < \frac{L_1}{L} + 1 \quad At \quad Y^* = \frac{H}{L}$$

$$\frac{\partial \Theta}{\partial Y^*} = 0 \quad \text{for} \quad \frac{L_1}{L} + 1 < X^* < \frac{L_1}{L} + \frac{L_2}{L} + 1 \quad \text{At} \quad Y^* = 0$$

## 2.4 stream function and vorticity formulation:

The governing two dimensional incompressible flow equations are given by Eqs.(5) to (7) are solved in stream function ( $\psi$ ) and vorticity ( $\omega$ ) formulation. The advantage of this formulation is that its adds to accuracy because it satisfies the mass conservation. It also reduces the number of unknowns to two as compared to three unknown in the primitive variable formulation

### 2.4.1 Stream Function

Stream function is defined as the Stream line to which velocity is tangent to every point. This is defined for a two dimensional flow. These are used to plot the stream lines, which are perpendicular to the equipotential lines.

The difference between the two stream function values gives the volumetric flow rate between the lines connecting the two points. Stream function is tangent to the velocity vector.

The stream function gives the direction of velocity in x and y direction with its partial derivative. It is represented as

$$\vec{V} = \nabla \times \Psi$$

In cartesian coordinate system this is equivalent to

$$u = \frac{\partial \Psi}{\partial y}; \quad v = -\frac{\partial \Psi}{\partial x}$$

Where u and v are the velocity in the x and y direction.. This also satisfies the conservation of mass equation .

## 2.4.2 Vorticity

The vorticity at a point is defined as the curl of velocity .In mathematical terms it can be written as.

$$\omega = \frac{\partial v}{\partial x} - \frac{\partial u}{\partial y} = -\nabla^2 \Psi$$

It is the amount of rotation or circulation in the fluid .When the viscous fluid flows the vorticity is produced by the viscous shearing action. It is proportional to the angular momentum of the fluid particle.Mathematically we can write it as

## 2.5 Vorticity transport equation

The Navier Stokes equation for incompressible fluid is to be solved by transforming to stream and vorticity formulation.The Pressure term is eliminated by differentiating the x momentum equation by y and y momentum equation by x and subtracting them.

We differentiate the x momentum equation with y and y momentum equation with x and subtracting them and further rearranging them we get

$$\begin{aligned} \frac{\partial}{\partial t^*} \left( \frac{\partial V^*}{\partial X^*} - \frac{\partial U^*}{\partial Y^*} \right) + U^* \frac{\partial}{\partial X^*} \left( \frac{\partial V^*}{\partial X^*} - \frac{\partial U^*}{\partial Y^*} \right) + V^* \frac{\partial}{\partial Y^*} \left( \frac{\partial V^*}{\partial X^*} - \frac{\partial U^*}{\partial Y^*} \right) = \\ \frac{1}{Re} \left\{ \frac{\partial^2}{\partial Y^{2*}} \left( \frac{\partial V^*}{\partial X^*} - \frac{\partial U^*}{\partial Y^*} \right) + \frac{\partial^2}{\partial X^{2*}} \left( \frac{\partial V^*}{\partial X^*} - \frac{\partial U^*}{\partial Y^*} \right) \right\} + \frac{Gr}{Re^2} \frac{\partial \theta}{\partial X^*} \end{aligned} \quad (2.12)$$

And substituting the value of  $\omega$  in the above equation we get the Vorticity Transport Equation

$$\frac{\partial \omega}{\partial t^*} + U^* \frac{\partial \omega}{\partial X^*} + V^* \frac{\partial \omega}{\partial Y^*} = \frac{1}{Re} \left( \frac{\partial^2 \omega}{\partial X^2} + \frac{\partial^2 \omega}{\partial Y^2} \right) + \frac{Gr}{Re^2} \frac{\partial \theta}{\partial X^*} \quad (2.13)$$

## 2.6 Orthogonal Transformation From x-y domain to $\xi - \eta$ domain

SFE, VTE and energy equation (EE) are further transform from(x,y)plane to obtain higher resolutionand easy implementation of boundary condition. The transformation from

(x,y) to  $(\xi, \eta)$  is given by

$$x(\xi) = x_{max} \left[ 1 - \frac{\tanh[\beta_1(1-\xi)]}{\tanh\beta_1} \right] \quad (2.14)$$

$$y(\eta) = y_{max} \left[ 1 - \frac{\tanh[\beta_1(1-\eta)]}{\tanh\beta_1} \right] \quad (2.15)$$

Where  $\beta_1 = 2.5$  is used to obtain a grid clustering near the surface to capture the gradients. So we have

$$\frac{\partial}{\partial x^*} = \frac{1}{h_1} \frac{\partial}{\partial \xi} \quad \frac{\partial}{\partial y^*} = \frac{1}{h_2} \frac{\partial}{\partial \eta} \quad (2.16)$$

where  $h_1$  and  $h_2$  are scale factors, where

$$h_1 = \left[ \left( \frac{\partial x}{\partial \xi} \right)^2 + \left( \frac{\partial y}{\partial \xi} \right)^2 \right] \quad h_2 = \left[ \left( \frac{\partial x}{\partial \eta} \right)^2 + \left( \frac{\partial y}{\partial \eta} \right)^2 \right]$$

The contra-variant components of velocity in the transformed plane are defined as,

$$h_2 u = \frac{\partial \psi}{\partial \eta} \quad \text{and} \quad h_1 v = -\frac{\partial \psi}{\partial \xi} \quad (2.17)$$

- Stream Function Equation

$$\frac{\partial}{\partial \xi} \left( \frac{h_1}{h_2} \frac{\partial \eta}{\partial \xi} \right) + \frac{\partial}{\partial \eta} \left( \frac{h_1}{h_2} \frac{\partial \Psi}{\partial \xi} \right) = -\omega h_1 h_2 \quad (2.18)$$

- Vorticity Transport Equation

$$h_1 h_2 \frac{\partial \omega}{\partial t^*} + \frac{\partial \Psi}{\partial \eta} \frac{\partial \omega}{\partial \xi} - \frac{\partial \Psi}{\partial \xi} \frac{\partial \omega}{\partial \eta} = \frac{1}{Re} \left( \frac{\partial}{\partial \xi} \left( \frac{h_1}{h_2} \frac{\partial \omega}{\partial \xi} \right) + \frac{\partial}{\partial \eta} \left( \frac{h_1}{h_2} \frac{\partial \omega}{\partial \eta} \right) \right) + \frac{Gr}{Re^2} \frac{\partial \Theta}{\partial \xi} \quad (2.19)$$

- Energy Equation

$$h_1 h_2 \frac{\partial \theta}{\partial t^*} + \frac{\partial \Psi}{\partial \eta} \frac{\partial \theta}{\partial \xi} - \frac{\partial \Psi}{\partial \xi} \frac{\partial \theta}{\partial \eta} = \frac{1}{Re Pr} \left( \frac{\partial}{\partial \xi} \left( \frac{h_1}{h_2} \frac{\partial \theta}{\partial \xi} \right) + \frac{\partial}{\partial \eta} \left( \frac{h_1}{h_2} \frac{\partial \theta}{\partial \eta} \right) \right) \quad (2.20)$$

## 2.7 Transformation of the Boundary Conditions From Physical Plane to the Computational Plane

- At the inlet and top of the domain free stream boundary conditions are applied as,

$$\text{At } x = 0 \text{ and } y = y_{max} : \Theta = \omega = 0; \quad \frac{\partial \psi}{\partial y} = h_2 \quad (2.21)$$

- Out Flow Condition the convective boundary condition are given by ,

$$\text{At } x = x_{max} : \frac{\partial v}{\partial x} = 0; \quad \frac{\partial \omega}{\partial x} = 0 \quad (2.22)$$

$$\frac{\partial T}{\partial x} = 0 \quad (2.23)$$

where  $u_c$  is the convection at the outflow taken as the free-stream velocity.No-slip boundary conditions on the surface for the velocity field are given by,

$$\text{At } y = 0 : \psi = \text{constant}, \quad \omega = -\frac{1}{h_2} \frac{\partial^2 \psi}{\partial \eta^2} \quad (2.24)$$

The boundary condition at the wall for temperature field is considered as constant heat flux on the heat source module and the rest of the plate is taken as adiabatic. The Boundary condition in dimensional form at the wall for temperature field are given by,

$$\frac{\partial \Theta}{\partial \eta} = 0 \quad \text{for } 0 < X^* < \frac{L_1}{L} \quad (2.25)$$

$$\frac{\partial \Theta}{\partial \eta} = -h_2 \quad \text{for } \frac{L_1}{L} < X^* < \frac{L_1}{L} + 1 \quad (2.26)$$

$$\frac{\partial \Theta}{\partial \eta} = 0 \quad \text{for } \frac{L_1}{L} + 1 < X^* < \frac{L_2}{L} + \frac{L_1}{L} + 1 \quad (2.27)$$

Where  $k$  is the thermal conductivity of the fluid;  $L_1$  is the distance between the leading edge point to the heat source ; $L$  width of the heat source; $L_2$  is the distance between from the end of the heat source module to end of the plate.



## 2.8 Nusselt Number

The heat transfer between the heat source module and the surrounding fluid is calculated in the form of a non-dimensional number, the Nusselt number (Nu). The local Nusselt number is calculated using the following equation

$$Nu_l = \frac{hL}{k} = \frac{qL}{k(T_s - T_\infty)} = \frac{1}{\theta_s \left(1 + 2.0\frac{H}{L}\right)} \quad (2.28)$$

The average Nusselt numbers ( $Nu_{avg}$ ) are obtained by integrating the local Nusselt number along the each sides of heat sources like left , top and right sides of heat source modules.

# Chapter 3

## Numerical Methods

In general the mathematical formulation of a physical problem involves a set of partial or differential equations that need to be solved in order to find an answer to the problem in question. However, the solution of these equations could be very complex, as in the case of a mixed convective flow described in previous chapter. In such cases the only way for finding an appropriate solution is via a numerical approach. Consequently to solve any problem by a numerical approach the mathematical formulation must be transformed by means of a discretization process to an easy format for the numeric process.

This means that the mathematical equations that are valid in the specific space and time or computational domain should be simplified to their equivalent forms in terms of an algebraic linear system of equations and then solved by approximations at definite points (discrete points) inside the computational domain. The greater the numbers of discrete points are added to the discretization of the domain, the numerical solution will approach the exact solution of the differential equations. However, to indiscriminately augment the number of discrete points would increase the round-off error.

Among the most frequent discretizing techniques used for fluid flow and heat transfer problems are the finite difference (FD), the finite element (FE), the finite volume (FV), and the spectral methods (SM).

In this thesis, the numerical discretization technique applied for solving the Navier-Stokes and the energy equations is the finite difference method. Finite difference methods approximate the solutions to differential equations by replacing derivative expressions

with approximately equivalent difference quotients. They are algebraic difference quotients which represent the various partial derivatives that occur in our governing equations. Hence, the solution of the governing partial differential equations involves the manipulation of algebraic quantities just the sort of operation that digital computers are designed to handle.

The Stream function equation (SFE), as given in the self-adjoint form, is discretized using second order central finite difference scheme as given in Anderson [14]. Vorticity transport equation (VTE) and Energy equation (EE) are solved by discretizing the diffusion terms in the same way as in the SFE. Time integration is performed by the four stage Runge-Kutta (Rk4) -scheme, and the nonlinear convection, terms are discretized by high accuracy compact schemes as give in sengupta[15].

SFE, VTE and EE equations are solved with 1000 points in the stream wise direction and 300 points normal to the flow direction using hyperbolic distribution to obtain grid clustering near the surface to capture velocity and temperature gradients. All simulations are obtained with double precision to reduce the round-off error.

# Chapter 4

## Flush mounted heat source modules results

Flush mounted heat sources means heat sources with negligible thickness and the heat source module to be flushed with the surface of the plate. Results are reported for single and double flush mounted heat sources with the same width  $L$ . Prandtl number value of air  $Pr = 0.7$  is taken for all simulations.

### 4.1 Single flush heat source module

Temperature, stream function and vorticity contours are shown in Figs 4.1 to 4.3 for forced convection flow with  $Re = 350$  with different stream wise grid points of 800 and 1000 . From Figs 4.1 to 4.3, one notice that solution is not changing much with increase of points 800 to 1000. The average nusselt number values for different points as shown in Table. 4.1. The average nusselt number value is almost equal with increase of points from 800 to 1000. This shows that solution is grid independent after 800 points. Here we have reported all results with 1000 grid points in the stream wise direction.

Table 4.1: Average Nusselt number and maximum surface temperature with different grid points for  $Re = 350$ ,  $Ri = 0.1$

S.No	Re	Ri	$Nu_{avg}(1000)$	$Nu_{avg}(800)$	Max Temp(1000 )	Max Temp(800 )
1	350	0.1	9.5753	9.5260	0.1544	0.1549

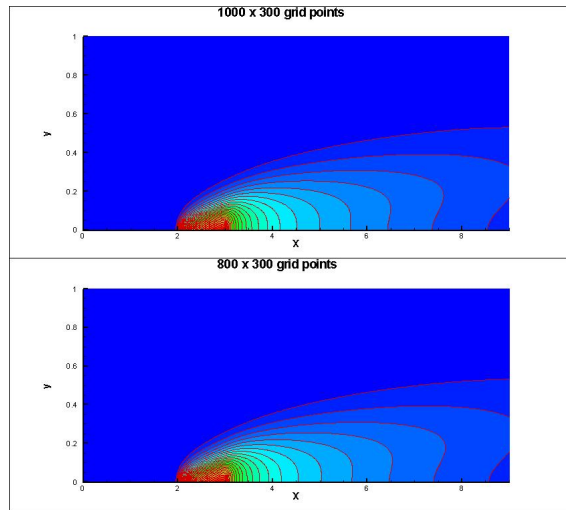


Figure 4.1: Temperature contours with different grid points

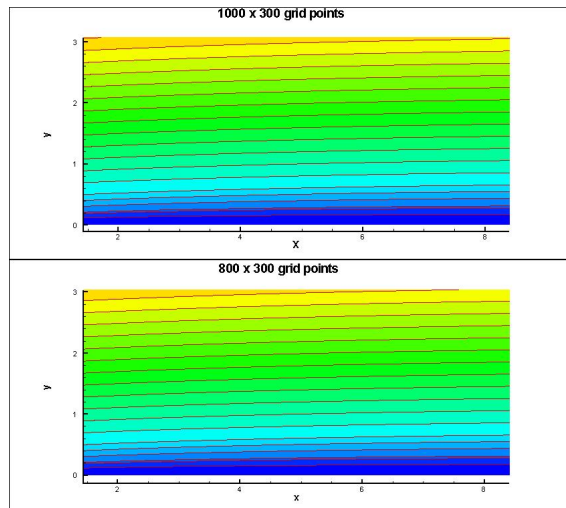


Figure 4.2: Stream Function contours with different grid points

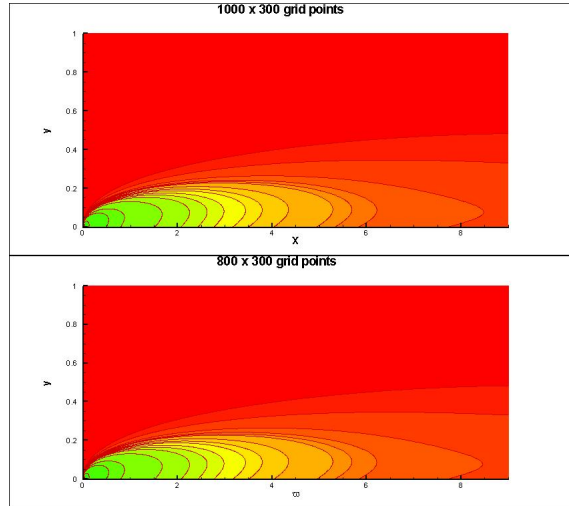


Figure 4.3: Vorticity contours with different grid points

First results are obtained for forced convection flow  $Ri = 0$  with Reynolds number  $Re = 350$ . Temperature, stream function and vorticity contours are shown in Figs. 4.4 to 4.6 with different dimensionless times  $t=5, 10, 15$  and  $20$ . The flush heat source location between  $x = 2$  to  $3$ . From Fig. 4.), the temperature contours are moving down stream with increasing of time means heat dissipating with time from the heat source. From Figs. 4.5 and 4.6, one can notice that velocity boundary layer is formed near surface and reaches the steady velocity boundary layer formation at  $t = 20$ .

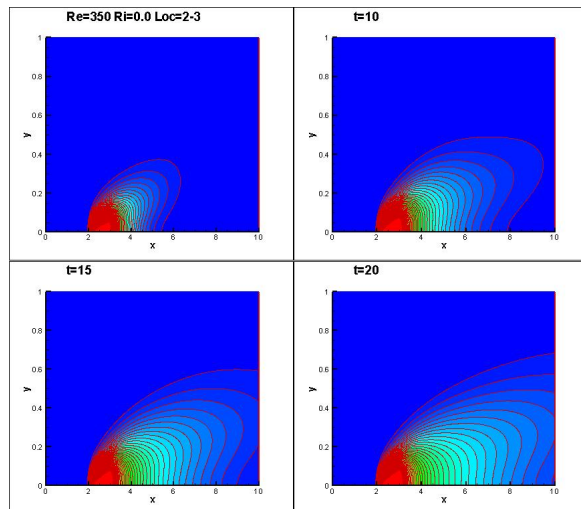


Figure 4.4: Temperature contours with different times for  $Re = 350$  and  $Ri = 0.0$

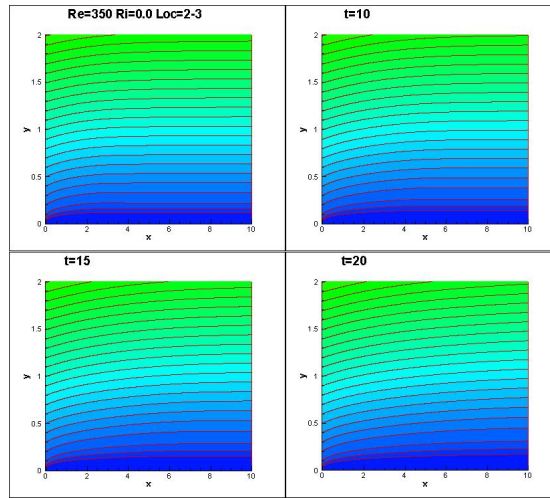


Figure 4.5: Stream Function Contours with different time for  $Re = 350$  and  $Ri = 0.0$

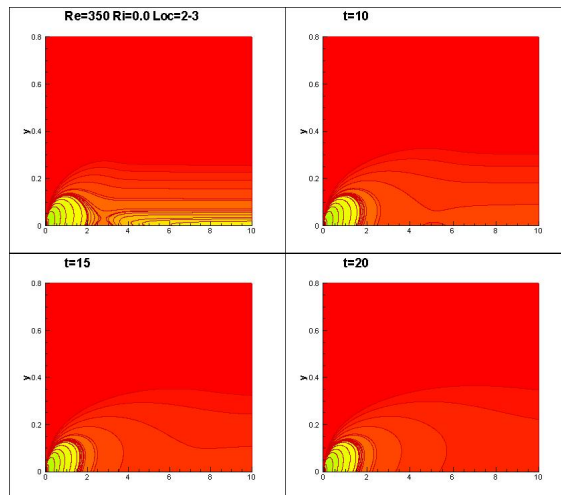


Figure 4.6: Vorticity Contours with different time for  $Re = 350$  and  $Ri = 0.0$

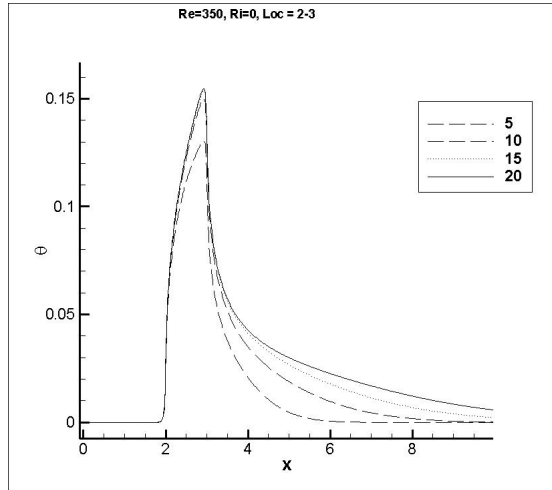


Figure 4.7: Surface Temperature with at  $t = 5, 10, 15$  and  $20$  for  $Re = 350$  and  $Ri = 0$

The surface temperature is shown in Fig 4.4 with different times for  $Re = 350$  and  $Ri = 0$ . From Fig. 4.4, the surface temperature increases with time and reaches steady state temperature at  $t = 20$ .

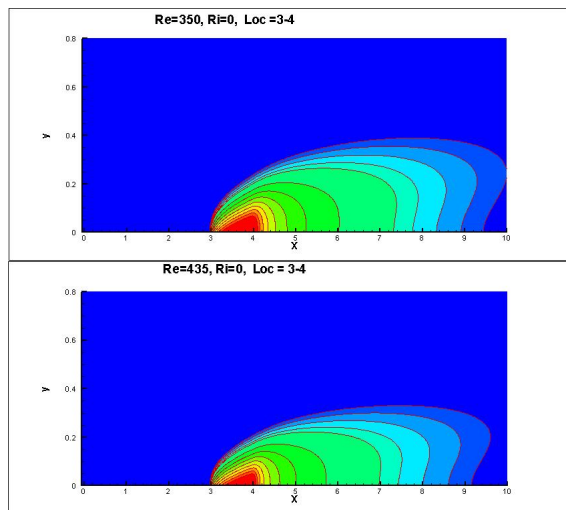


Figure 4.8: Surface temperature contour different Reynolds Number for  $Ri = 0$  and  $Loc = 2 - 3$

Steady state temperature contours and surface temperature are shown in Figs 4.8 and 4.9 for  $Re = 350$  and  $435$  with  $Ri = 0$  and location 3 to 4. From Figs, 4.8 and 4.9 shows that temperature values decreases with increasing  $Re$ . As the Reynolds number increases the temperature values are decreases means faster cooling of heat source which



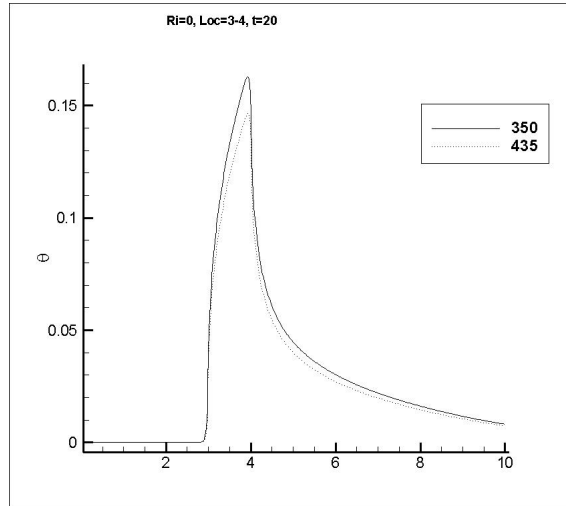


Figure 4.9: Surface temperature with different Reynolds Number for  $Ri = 0$  and  $Loc = 3$  - 4

corresponds physically one expects that heat source module cools faster as the free stream velocity increases. This shows one of validation of present results.

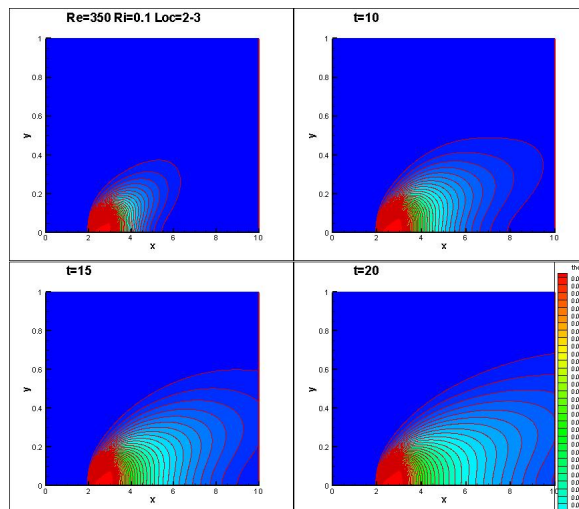


Figure 4.10: Temperature contours with different times for  $Re = 350$  and  $Ri = 0.1$

Mixed convection flow results are obtained for the case of  $Re = 350$  and  $Ri = 0.1$ . The location of the flush heat source between  $x = 2$  to  $3$ . Temperature, stream function and vorticity contours are shown in Figs 4.10, 4.11, and 4.12 with different dimensionless times  $t = 5, 10, 15$  and  $20$ . From Figs 4.10, to 4.12 mixed convection flow results shown

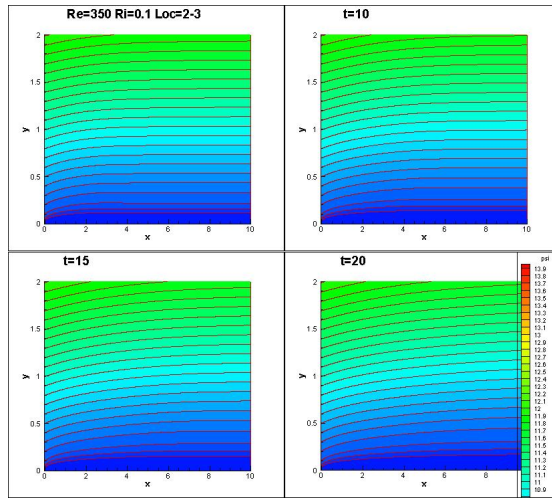


Figure 4.11: Stream function contours with different times for  $Re = 350$  and  $Ri = 0.1$

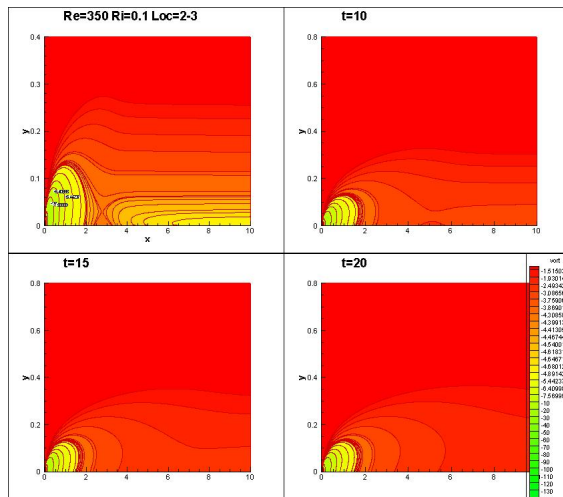


Figure 4.12: Vorticity contours with different times for  $Re = 350$  and  $Ri = 0.1$

the same trend of forced convection  $Ri=0$  results as shown in Figs 4.4 to 4.6.

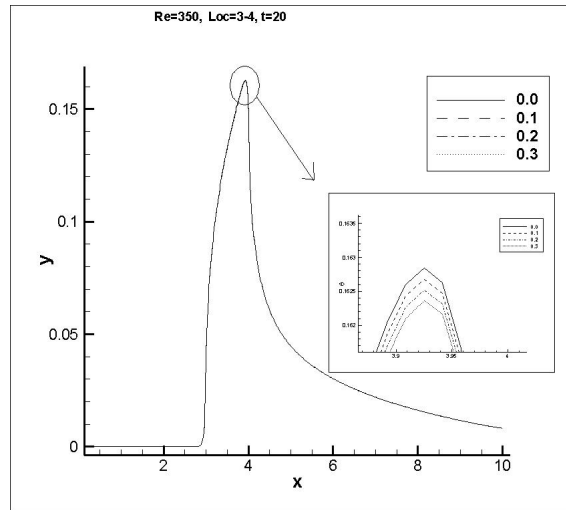


Figure 4.13: Surface temperature with different Richardson number for  $Re = 350$

The steady state surface temperature is shown in Figs. 4.13 for  $Re = 350$  with different Richardson number values  $Ri = 0, 0.1, 0.2$  and  $0.3$ . From Figs. 4.13 the surface temperature decreases very small with increase of  $Ri$ . As  $Ri$  increases, flow becomes unstable and increases the convective heat transfer coefficient which corresponds surface temperature decreases. The flow becomes unstable as  $Ri$  increases for mixed convection flow over a horizontal plate as reported in Venkatasubbaiah [13]. Very small change of non-dimensional surface temperature with increasing  $Ri$  physical shows significant change of surface temperature on the heat source.

The steady surface temperatures of forced convection flow  $Ri = 0.0$  are shown in Fig. 4.14 for  $Re = 350$  with different flush heat source locations between  $x = 2$  to  $3$ ,  $3$  to  $4$ , and  $5$  to  $6$ . From Fig. 4.14, the surface temperature increases with increase of heat source location because increasing the distance from the leading edge leads to increase the thickness of boundary layer which corresponds decrease in convective heat transfer coefficient  $h$ . As  $h$  decreases for the same amount of heat dissipated by heat source correspondingly increase the surface temperature of the heat source.

Fig. 4.15 also shows the the steady state temperature for mixed convection flow for  $Ri = 0.1$  with  $Re = 350$  and flush source location between  $2$  to  $3$ ,  $4$  to  $5$ ,  $6$  to  $7$ , and  $7$  to  $8$ . This also shows that the surface temperature increases as the distance of flush source

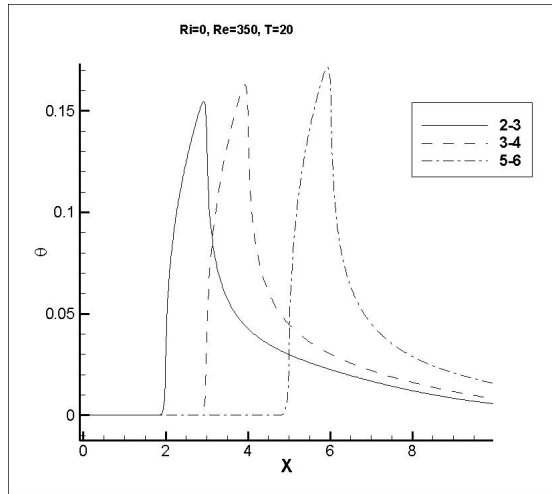


Figure 4.14: Surface temperature with different Flush source location for  $Ri = 0.0$

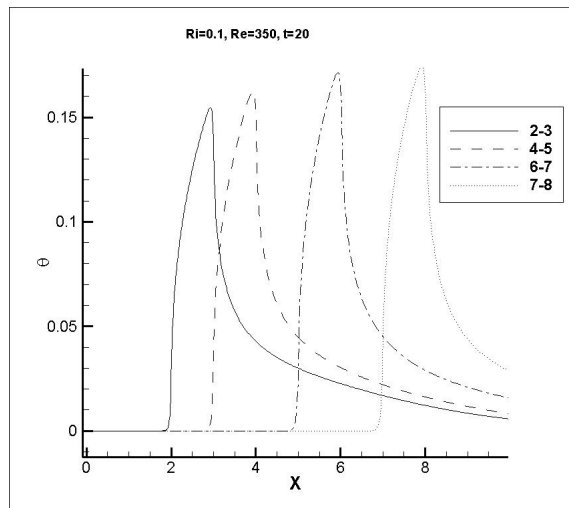


Figure 4.15: Surface temperature with different Flush source location for  $Ro = 0.1$

Table 4.2: Maximum surface temperature and average Nusselt number values for flush source modules

S.no	Re	Ri	Loc	$\theta$	Nu(avg)
2	350	0	2-3	0.15005	9.56713
3	350	0	3-4	0.15338	8.8465
4	350	0	5-6	0.17138	8.13302
5	435	0	4-3	0.14646	9.89934
6	350	0.1	2-3	0.15414	9.57532
7	350	0.1	3-4	0.16254	8.85628
8	350	0.1	5-6	0.17123	8.14428
9	435	0.1	7-8	0.19817	7.83457
10	350	0.2	3-4	0.16254	8.86577
11	435	0.2	3-4	0.14646	9.89934
12	350	0.3	3-4	0.16225	8.87532

module from leading edge.

The average Nusselt number and maximum surface temperature values for all the cases are shown in Table 4.2. From Table 4.2, The average nusselt number values are increases with increase of Re because increase of free stream velocity correspondingly increase of convective heat transfer coefficient. The average Nusselt number decreases with increase of Ri at a fixed Re due to the flow becomes unstable. The average Nusselt number decreases with increase of heat source location from the leading edge due to increase of boundary layer thickness.

## 4.2 Double flush heat source modules

Fig. 4.16 to 4.18 shows the plots for temperature contours, vorticity contours and stream function contours for the case Reynolds Number,  $Re = 350$ , Richardson Number,  $Ri = 0.1$  with heat source location at 2 to 3 and 4 to 5. In Fig. 4.16 the temperature contours moves downstream with the increase in time because of more heat in the flow field. The location of the maximum temperature is above the right corner of the flush source .

In Fig. 4.17 we can see the vorticity is highest at the left corner which slowly dissipates in the downstream. The plate leading edge act as source for the vorticity generation.

Fig. 4.18 shows the stream function plots in the flow field. It shows initially the

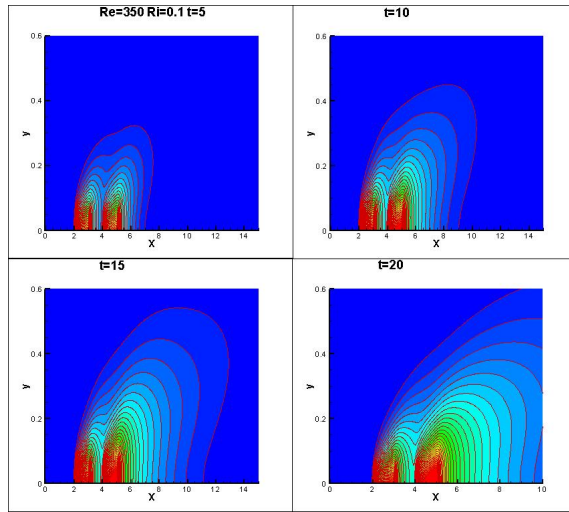


Figure 4.16: Nondimensionlazed Temperature contours in flow field for different time

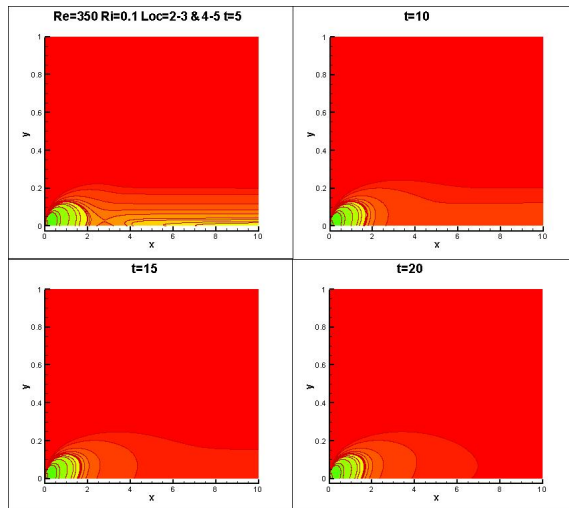


Figure 4.17: Vorticity contours in flow field for different time

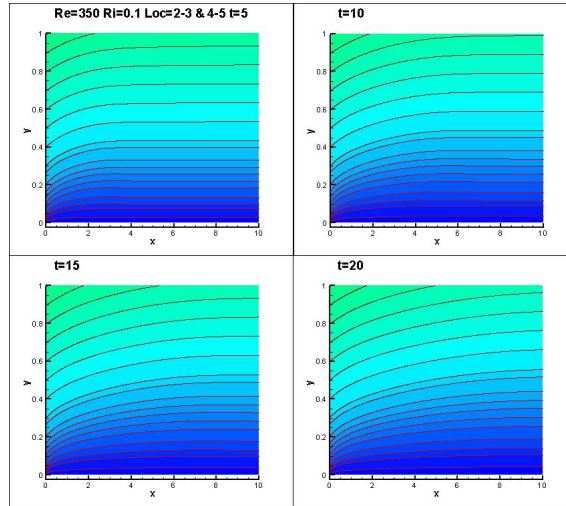


Figure 4.18: Stream Function in flow field for different time

contours are almost parallel to the plate showing fluid velocity has only x component. But with time due to heating there is a upward motion in the fluid due to the density difference. And hence it raises up giving velocity in y direction and making the stream function curved.

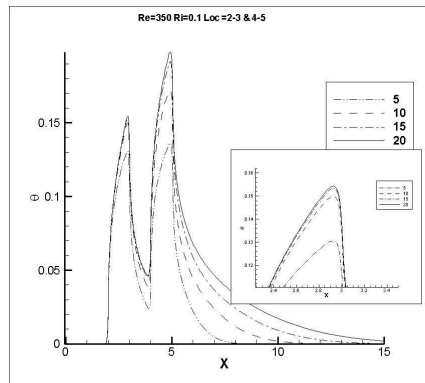


Figure 4.19: Surface temperature for different Re for,  $Ri = 0.1$  at  $t=20$

The surface temperature is shown in Fig. 4.19 with different times for  $Re = 350$  and  $Ri = 0.1$  with heat source location at 2 to 3 and 6 to 7. From Fig. 4.19, the surface temperature increases with time and reaches steady state temperature at  $t = 20$ . We have assumed the same amount heat dissipated by the heat source 1 and heat source 2. From Fig. 4.1), the surface temperature of second heat source is higher compared to

the first heat source due to the increase of boundary layer thickness from the first source to the second source. As the thickness of boundary layer increases leads to decrease of convective heat transfer coefficient which corresponds increase of surface temperature.

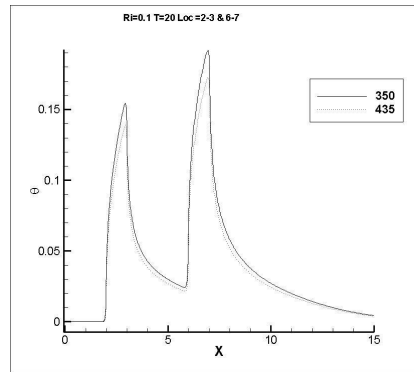


Figure 4.20: Surface temperature for different Re for,  $Ri = 0.1$  at  $t=20$

Fig. 4.20 shows the effect of Reynolds Number on the Surface temperature over the plate. The cases plotted are for Richardson Number,  $Ri = 0.1$  with flush source location at 2 to 3 and 6 to 7. The plots shows that there is a decrease in the surface temperature with increase in the Reynolds Number over both heat source. This happens because with increase in the Reynolds number the velocity of the fluid increase and hence more heat removal takes place.

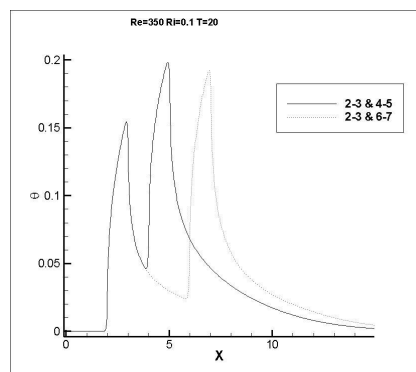


Figure 4.21: Surface temperature for different heat source location for,  $Ri = 0.1$  at  $t=20$

The surface temperature is shown in Fig. 4.21 with different locations for  $Re = 350$  and  $Ri = 0.1$ . The first heat source is located at  $x = 2$  to  $3$  while the second heat sources



Table 4.3: Maximum surface temperature and average Nusselt number values for two flush heat source modules

S.no	Re	Ri	Loc	$\theta$	Nu(avg)
1	350	0	2-3	0.15452	9.57651
			6-7	0.19190	6.72612
2	350	0.1	2-3	0.15445	9.5849
			6-7	0.19174	6.73317
3	435	0.1	2-3	0.13525	10.7235
			6-7	0.17268	6.51486
4	350	0.1	2-3	0.14995	9.58529
			4-5	0.19817	6.30209

are located at the  $x = 4$  to  $5$  and  $6$  to  $7$ . From Fig. 4.21, the surface temperature increases with increase of heat source location because increasing the distance from the leading edge leads to increase the thickness of boundary layer which corresponds decrease in convective heat transfer coefficient  $h$ . As  $h$  decreases for the same amount of heat dissipated by heat source correspondingly increase the surface temperature of the heat source. From Fig. 4.21, one can notice that the maximum surface temperature over the second heat source is increases with decrease of distance between two heat sources due to the increase of interaction between two heat sources.

From Table 4.3, The average nusselt nubner values are increases with increase of  $Re$  because increase of free stream velocity correspondingly increase of convective heat transfer coefficient. The average  $Nu$  values are decreases with increase of heat source location from the leading edge due to increase of boundary layer thickness. The maximum surface temperature over the second heat source is increases with decrease of distance between two heat sources due to the increase of interaction between two heat sources.

# Chapter 5

## Heat source modules with thickness

### 5.1 Single heat source module with thickness

The temperature contours of mixed convection flow over heat source module are shown in Fig. 5.1 for  $Re = 350$  and  $Ri = 0.1$  with different times at  $t = 5, 10, 15$  and  $20$ . The thickness and location of heat source module are  $H/L = 0.25$  and location  $x = 2$  to  $3$ . As the time increases the contours get extended in the down stream direction. This is because the heat is being convected in the same direction of fluid flow. One peculiar property we see that there is no much effect in the upstream plate .ie the temperature remains unaffected .

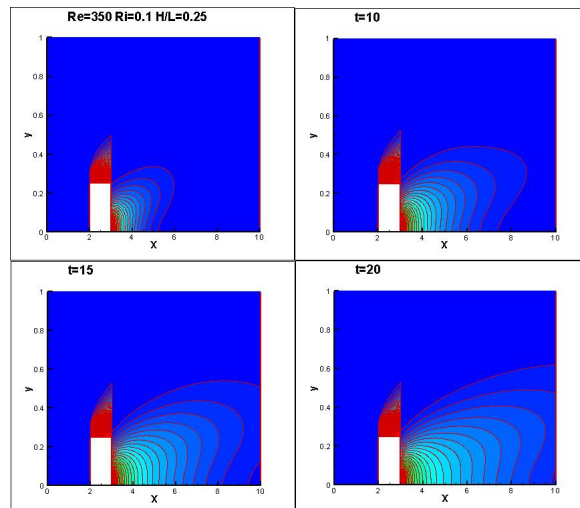


Figure 5.1: Temperature contours at  $t = 5, 10, 15$  and  $20$

Fig. 5.2 shows the zoomed view around the heat source for the above case. It shows the location of the maximum temperature above the heat source which is near right side from the centre of the top face of the heat source module.

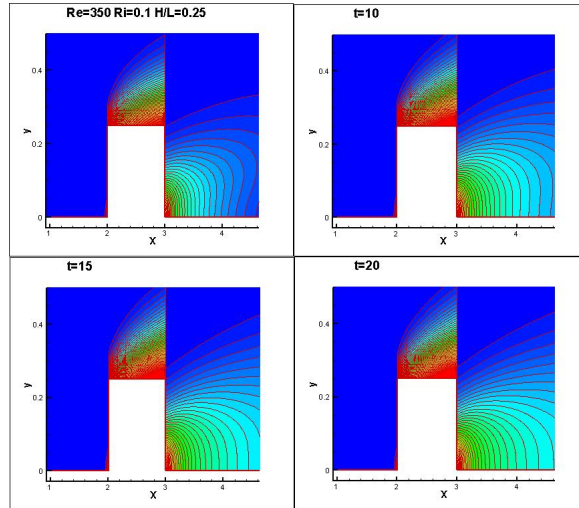


Figure 5.2: Zoomed view of Temperature contours near heat source modules at  $t = 5, 10, 15$  and  $20$

Fig. 5.3 shows the vorticity plot of the flow field for the same case,  $Re = 350, Ri = 0.1, H/L = 0.25$  with heat source location 2 to 3. Initially we see that the leading edge is the source of the vorticity. This slowly propagates and eventually dies out. Fig 5.4 gives the stream function of the flow field for the same case. Initially we see that stream lines are almost horizontal to the plate. But with time increases as the vertical velocity of the air starts increases due to buoyancy force and then the stream function becomes curved.

The surface temperature of the heat source module is shown in Fig. 5.5 for  $Re = 350$  and  $Ri = 0.1$  with different times  $t = 5, 10, 15$  and  $20$ . As the time increases the surface temperature of the heat source module increases and reaches the steady state value at  $t=20$ . From Fig. 5.5, the maximum temperature reaches at the right corner of heat source.

Fig. 5.6 shows the variation of the surface temperature due to change in the Richardson number. In this figure the isothermal lines are shown for the  $Re = 350, H/L = 0.25$  with heat source location at  $x = 2$  to  $3$ . The cases considered are  $Ri = 0, 0.1$  and  $0.3$ . From Fig. 5.6 the surface temperature decreases with increase of  $Ri$  at a fixed  $Re$  because the flow becomes unstable due to buoyancy. As  $Ri$  increases, convective heat transfer

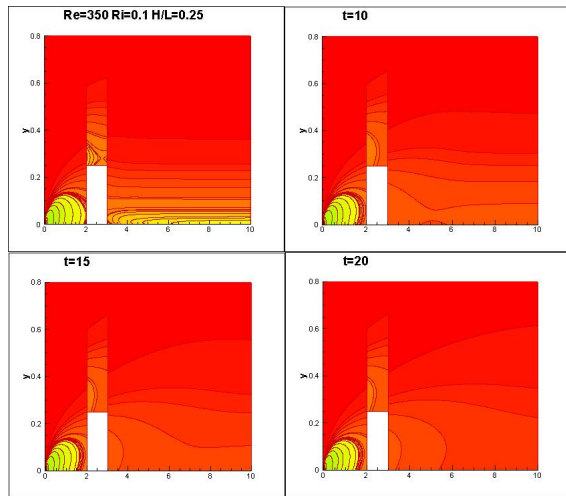


Figure 5.3: Vorticity contours at  $t = 5, 10, 15$  and  $20$

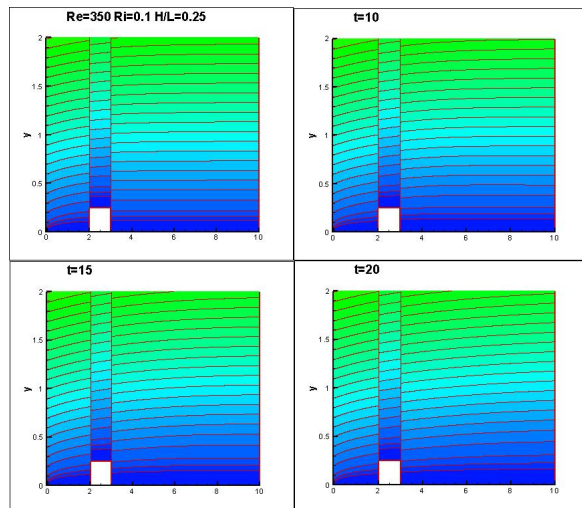


Figure 5.4: Stream function contours at  $t = 5, 10, 15$  and  $20$

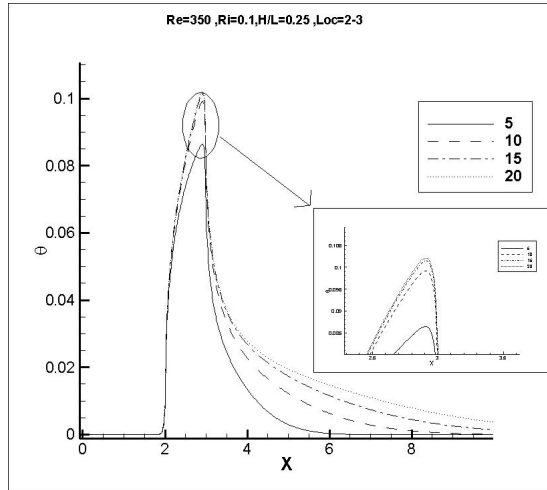


Figure 5.5: Surface temperature at  $t = 5, 10, 15$  and  $20$

coefficient increases due to buoyancy and the surface temperature decreases for constant heat flux emitted by the heat source. The non-dimensional surface temperature of the heat source slightly decreases with  $Ri$  but physically significant change of dimensional surface temperature of the heat source.

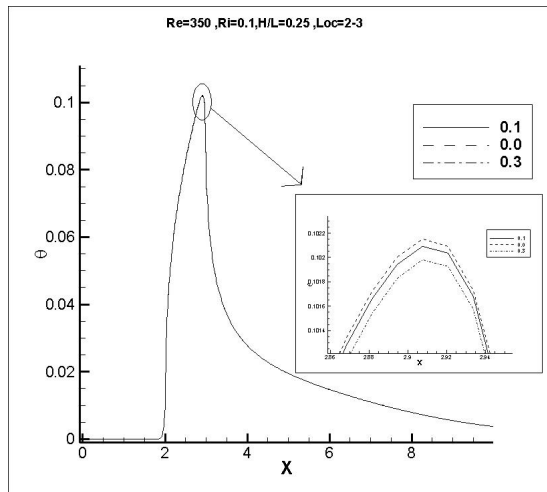


Figure 5.6: Effect of Richardson number on Surface temperature for  $Re = 350$  and  $H/L = 0.25$

Fig. 5.7 shows the vorticity plots in the flow field. The vorticity plots are almost same showing least affected by the Richardson Number.

The Fig. 5.8 shows the effect of the Reynolds number on the surface temperature.

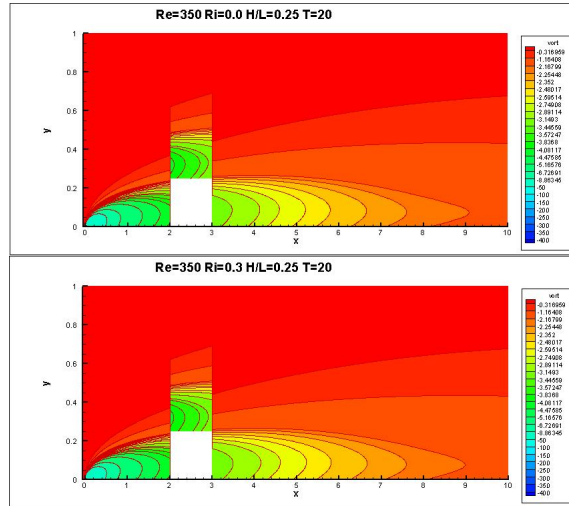


Figure 5.7: Effect of Richardson number on Vorticity contours for  $Re = 350$  and  $H/L = 0.25$

In Fig. 5.8 isotherm lines are shown for the fixed Richardson number,  $Ri = 0.1$ , source thickness,  $H/L = 0.25$ , and fixed location, 2 to 3 for the three values of Reynolds Number,  $Re = 350, 435$  and  $830$ . With the increase in the Reynolds Number the boundary layer above the heat source keeps decreasing. This is obvious as the fluid velocity increases with the Reynolds number. This leads to higher coefficient of heat transfer leading to the more heat dissipation and bring down the temperature further down.

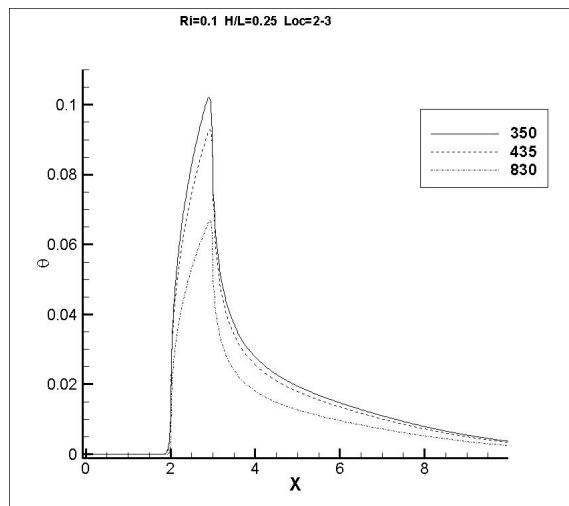


Figure 5.8: Effect of Reynolds number on surface temperature for  $Ri = 0.1$  and  $H/L = 0.25$

The effect of Reynolds in the flow field can be further observed in the Fig. 5.9. The figure shows the isothermal lines distribution in the flow field for different Reynolds Number ,Re = 835 and 435. Other condition are Ri = 0.1, H/L= 0.25 at t = 20. It shows that the temperature contours shrink further with increase in the Reynolds number. Fig. 5.10 shows the temperature contours for Re = 835 and 435 with Ri = 0.1, and H/L = 0.25 at t = 20.

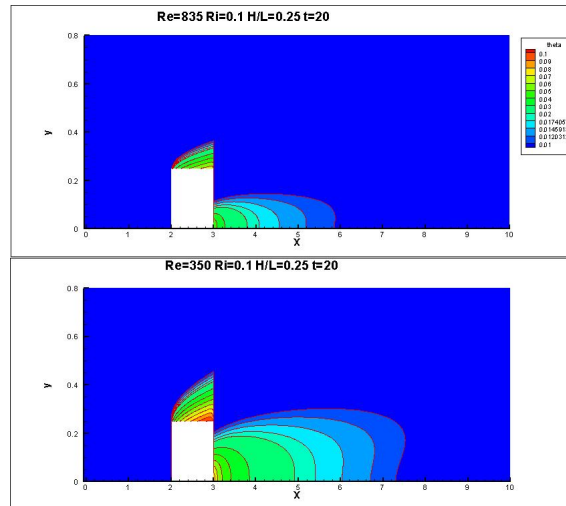


Figure 5.9: Effect of Reynolds number on temperature contours for Ri = 0.1 and H/L = 0.25

The Fig 5.11 shows the vorticity distribution for different Reynolds number Re=350 and 835 with Ri=0.1 and H/L=0.25 .For higher Reynolds the vorticity generation is high at the surface and dissipates downstream of the heat source module and also certain distance of the upstream of the heat source module.This causes the more viscous and heat dissipation and hence bringing down the surface temperature of heat source module

Fig. 5.12 also shows the vorticity distribution comparison for two different Reynolds number Re = 835 and 350 for Richardson Number, Ri = 0.1 and heat source thickness, H/L = 0.25. It shows that the vorticity is higher in the downstream to the left of the flush source. The vorticity above and to the left surface of the flush source is also higher at high Reynolds Number.

Figs. 5.13 and 5.14 shows the effect of the location of heat source on the surface temperature. In Fig. 5.13, the results are shown for Re = 350, Ri = 0.1 , and H/L =

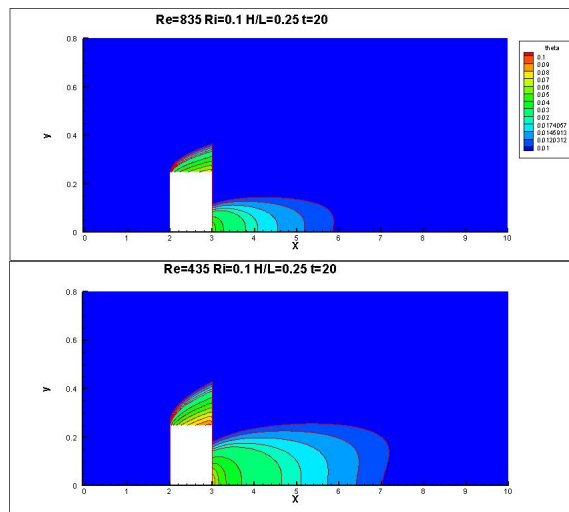


Figure 5.10: Effect of Reynolds number on temperature contours for  $Ri = 0.1$  and  $H/L = 0.25$

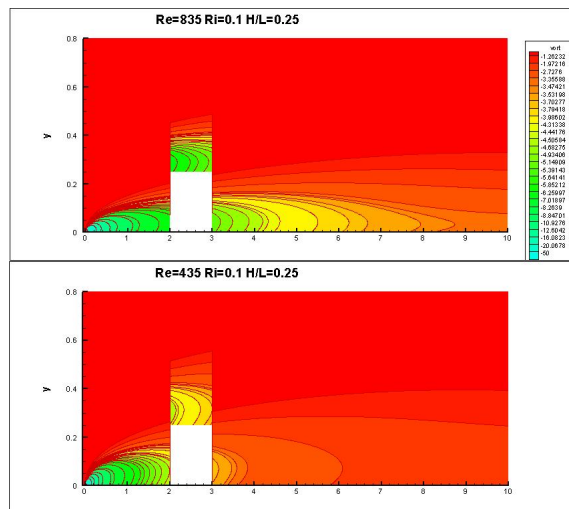


Figure 5.11: Effect of Reynolds number on vorticity contours for  $Re = 435$  and  $835$



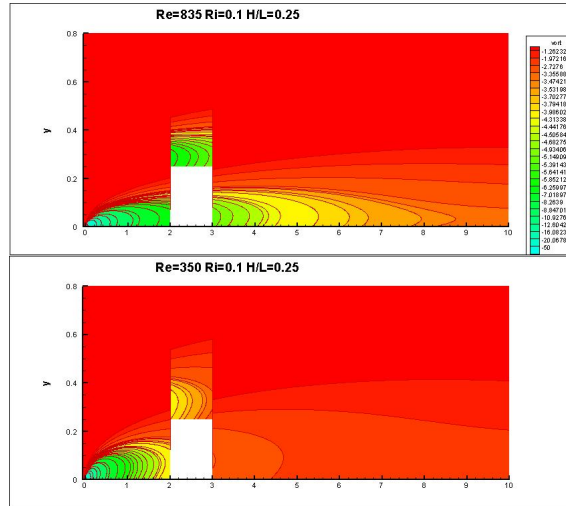


Figure 5.12: Effect of Reynolds number on vorticity contours for  $Re = 350$  and  $835$

0.25. The heat source location are 2 to 3 and 4 to 5 . In Fig. 5.14 results are given for the  $Re = 350$ ,  $Ri = 0.1$  and  $H/L = 0.5$ . The heat source is located at 2 to 3 and 4 to 5. The maximum temperature increases as the source is moved away from the leading edge. As the boundary layer thickness above the heat source away from the leading edge is more, so the heat transfer coefficient is value is less and hence higher temperature. This happens because with the increase in the boundary layer thickness there is a decrease in the heat transfer coefficient. So, heat source module location at 4 to 5 lies in the thicker zone that leads to lower  $h$  value.

Figs. 5.15 and 5.16 shows the vorticity pattern above the plate and around heat source for different Reynolds Number. It shows high vorticity on all three surface of the heat source .ie left ,top and right surface .This leads to the high heat dissipation of heat above the heat module and hence lowering the temperature.

The surface temperature is shown in Fig. 5.17 with different thickness of the heat source module for  $Re = 350$  and  $Ri= 0$ . The location of the heat source is  $x = 2$  to  $3$ . The different thickness are  $H/L = 0.0, 0.25$  and  $0.5$ . From Fig. 4.17, one can notice that the surface temperature decreases drastically with the increase of heat source thickness due to increase of surface area. The surface temperature decreases with the increase of surface area due to constant heat input of the heat source. This shows that thickness of heat source module is most important parameter while design of thermal system for

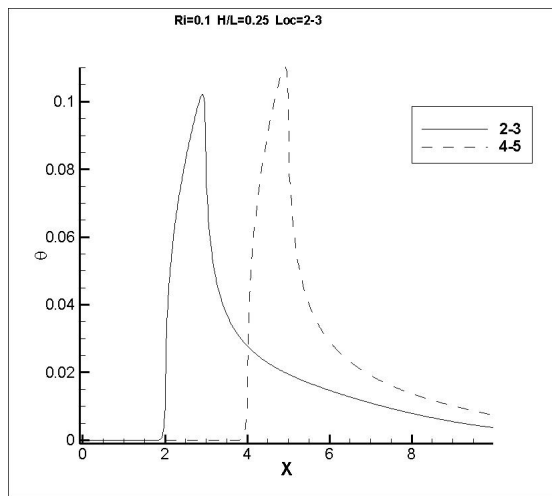


Figure 5.13: Effect of location on heat source module on surface temperature for  $H/L = 0.25$  and  $Re = 350$

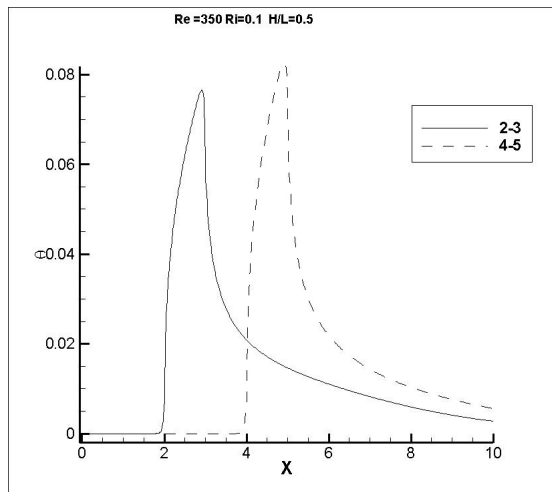


Figure 5.14: Effect of location on heat source module on surface temperature for  $H/L = 0.50$  and  $Re = 350$

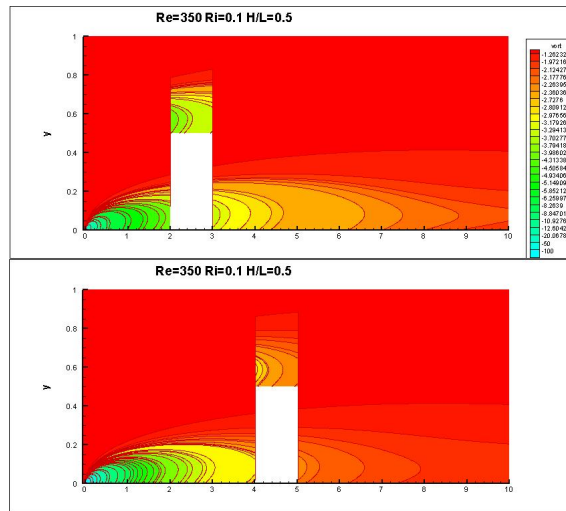


Figure 5.15: Effect of location on heat source module on vorticity contours for  $H/L = 0.25$  and  $Re = 350$

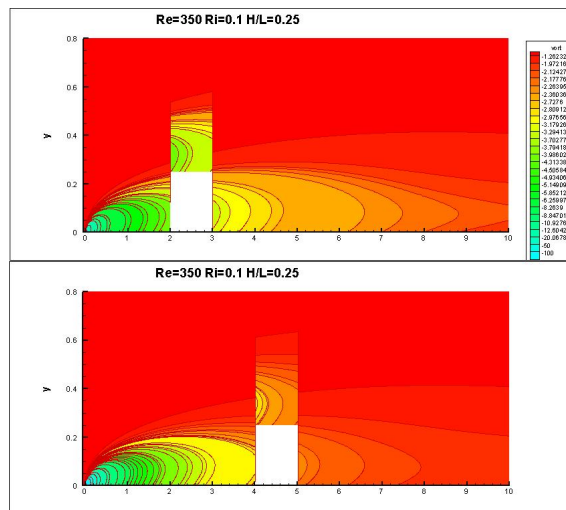


Figure 5.16: Effect of location on heat source module on vorticity contours for  $H/L = 0.50$  and  $Re = 350$

cooling of electronic devices.

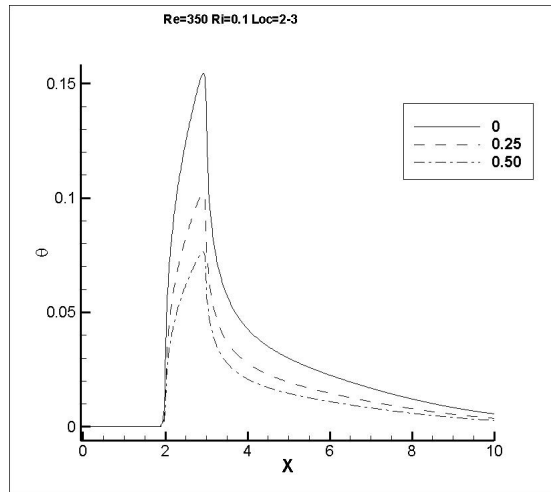


Figure 5.17: Effect of thickness on heat source module on surface temperature for  $Ri = 0.1$  and  $Re = 350$

The surface temperature of mixed convection flow is shown in Fig.5.18 with different thickness of the heat source module for  $Re = 350$  and  $Ri = 0.1$ . The location of heat source is  $x = 2$  to  $3$ . The different thickness are  $H/L = 0.0, 0.25$  and  $0.5$ . From Fig. 5.18, one notice that the surface temperature profile for mixed convection flow shows the same trend of forced convection flow as shown in Fig. 5.17 with different thickness of heat source.

The vorticity contour values are slight change and pattern is same with increase of thickness.

The average Nusselt number values of each face of heat source module means left, top and right face of the heat source module are obtained and shown in Table 5.1. The maximum surface temperature of the heat source module as shown in Table 5.1. From Table, one can notice that the Nusselt number value is high for left face of the heat source and low for right face of heat source module. The Nusselt number value of the top face is lies between left and right faces. From Fig. 5.5, one can notice that the surface temperature suddenly increases and reaches a maximum value and then decreases along the faces of the heat source module due to energy input of the heat source module. So the local convective heat transfer coefficient also suddenly increases along the left face and

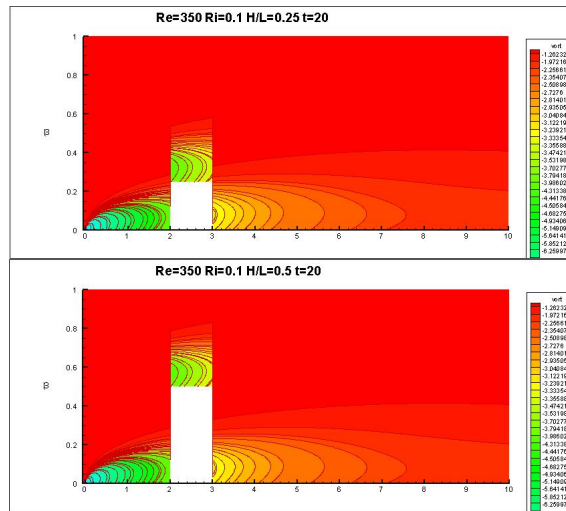


Figure 5.18: Effect of thickness on heat source module on Vorticity contours for  $Ri = 0$  and  $Re = 350$

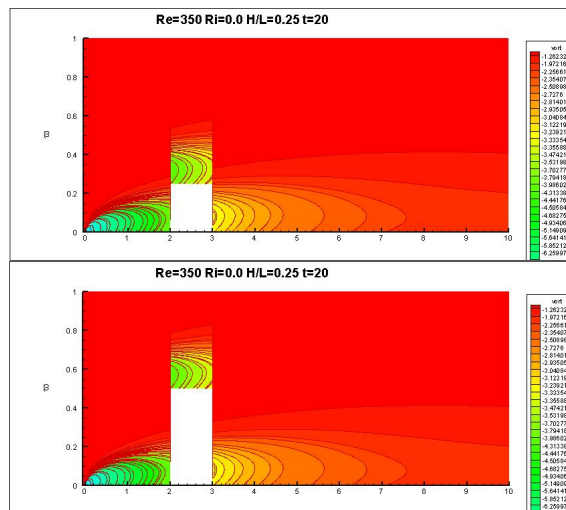


Figure 5.19: Effect of thickness on heat source module on surface temperature for  $Ri = 0.1$  and  $Re = 350$

Table 5.1: Plate with single heat source modules

S.no	Re	Ri	H/L	Loc	Nu(L.F)	Nu(T.F)	Nu(R.F)	$\theta$
1	350	0.0	0.25	2-3	38.4870	6.9913	5.6745	0.1021
2	350	0.0	0.50	2-3	28.8652	5.2435	4.2559	0.07659
3	350	0.1	0.50	2-3	28.8856	5.2458	4.2575	0.07655
4	350	0.1	0.25	2-3	38.5231	6.9955	5.6769	0.10204
5	350	0.1	0.50	4-5	29.0647	4.8753	4.0557	0.08300
6	350	0.1	0.25	4-5	38.7693	6.5286	5.4083	0.11503
7	435	0.1	0.25	2-3	30.6939	7.4119	5.6269	0.0927
9	835	0.1	0.25	2-3	112.4526	11.7166	8.6151	.0699
11	830	0.1	0.50	2-3	83.6259	8.7536	6.4423	
10	835	0.1	0.25	4-5	132.6456	11.7598	8.2145	0.7267
11	350	0.3	0.25	2-3	38.5952	7.0038	5.6815	0.10197

slowly decreases till right face of the heat source module due energy input of heat source. Same trend of average Nusselt number values along the faces of heat source module are found experimentally and given in Kang *et al* [11]. From Table 5.2 , The average Nusselt number values are good agreement with the experimental results given by Jaluria et al [number] for the case of  $Re = 435$ ,  $Ri = 0.6357$  and thickness of heat source module  $H/L = 0.28$ . Present Nu values are valid for forced convection dominated flows only. Present Nu values are not exactly matching with the Kang *et al* [11] results due to the following reason:

- They have conducted experiment for high values of Grashoff number and low values of Reynolds number means that natural convection flow is more dominated compared to forced convection effects

From Table. 5.1 , The average Nusselt values are decreases with the increase of location of the heat source from the leading edge due to increase the boundary layer thickness. The average Nusselt number values decreases with increase the thickness of the heat source due to increase of surface area for the same energy input to the heat source.

## 5.2 Double heat source modules with thickness

Fig. 5.20 gives the surface temperature distribution on the plate for  $Re = 350$ ,  $Ri = 0.1$ ,  $H/L = 0.25$  with heat source location 2 to 3 and 4 to 5 for the non-dimension time  $t =$

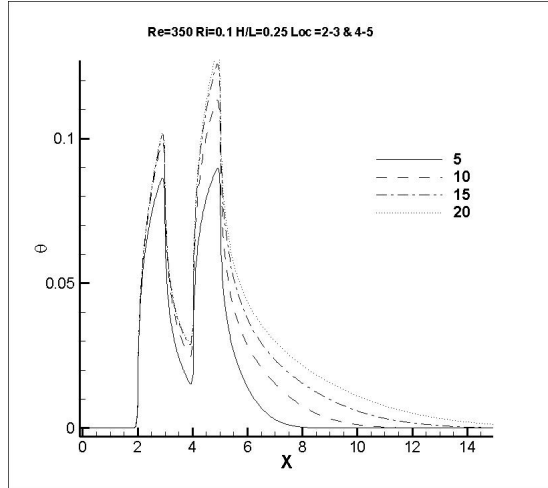


Figure 5.20: Surface temperature at  $t=5, 10, 15,$  and  $20$

5, 10, 15 and 20. It shows the surface temperature above the second heat source is more than the first heat source. As heat is convected towards the right this further increase the temperature above the heat source. The rate of increase of the temperature also decreases with the time. And also the heat transfer coefficient is higher for the first heat source than the second heat flush due to thicker boundary layer above the second heat source.

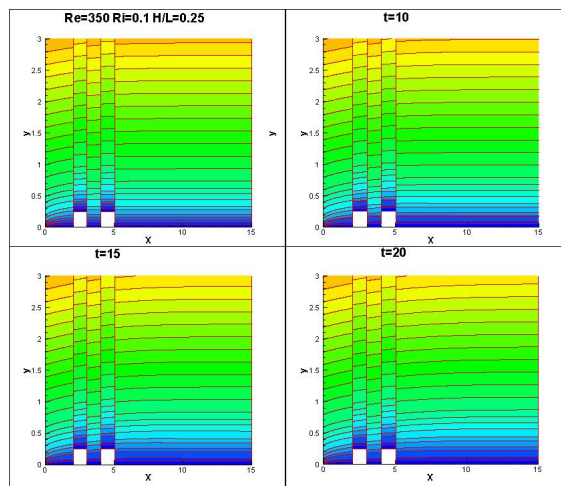


Figure 5.21: Stream function contours at  $t = 5, 10, 15$  and  $20$

Fig. 5.21 gives the stream function contours in the flow field for the same case for different non dimensionless time  $t= 5, 10, 15$  and  $20$ .

Fig. 5.22 shows the vorticity contours in the flow field for the above case. As we

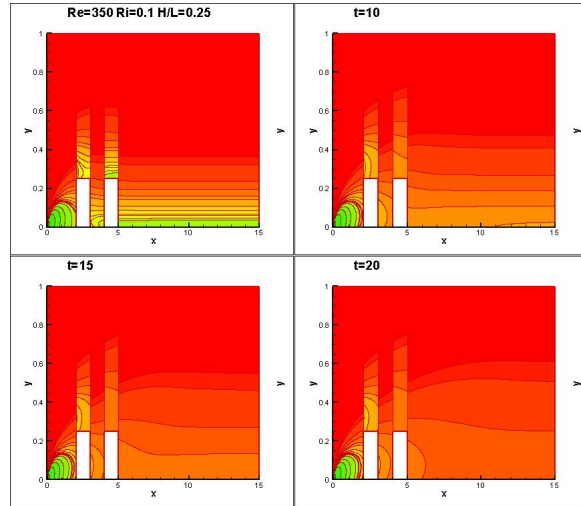


Figure 5.22: Vorticity contours at  $t = 5, 10, 15$  and  $20$

saw in single flush source we see that leading edge of the plate is source of vorticity generation. The vorticity initially above the second heat source is high and slowly this vorticity dissipates in the field. Initially the vorticity generation above the second heat source is higher than the first source.

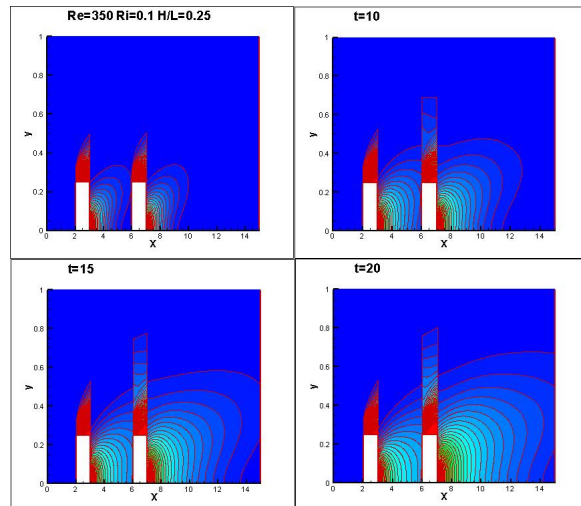


Figure 5.23: Temperature contours at  $t = 5, 10, 15$  and  $20$

Fig. 5.23 gives the temperature contours for the flow region. The location of maximum temperature is above the second heat source. With time as more heat input is there given the thickness of the boundary layer increases.



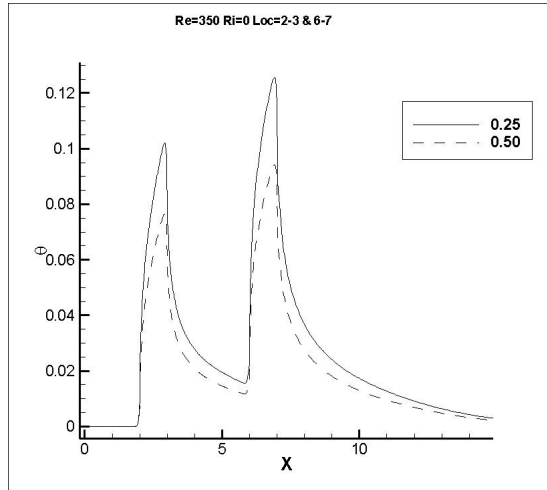


Figure 5.24: Effect of heat module thickness on surface temperature for  $Ri = 0$

Fig. 5.24 shows the effect of the thickness of heat source on the surface temperature for the Reynolds Number,  $Re = 350$ , Richardson Number,  $Ri = 0$  and flush source location 2 to 3 and 6 to 7. As observed earlier The surface temperature decreases with increase of thickness due to increase of surface area for the same energy input to the heat source.

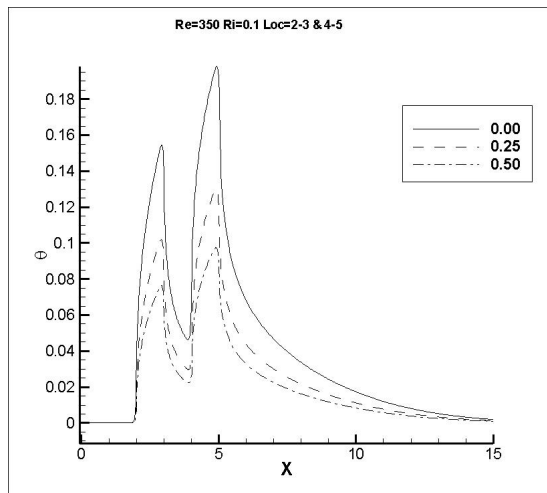


Figure 5.25: Effect of heat module thickness on surface temperature for  $Ri = 0.1$

Fig. 5.25 also shows the effect of the thickness on the heat source. The plots are plotted for the thickness  $H/L = 0, 0.25$  and  $0.50$  for the case  $Re = 350, Ri = 0.1$  with heat source location  $x = 2$  to  $3$  and  $4$  to  $5$ . As expected the temperature is coming down with increase in the thickness of the heat source due to increase of surface area.

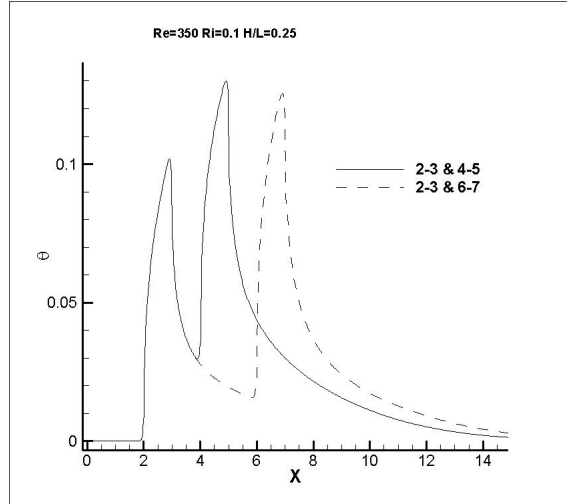


Figure 5.26: Effect of space between heat source module on surface temperature for  $Ri = 0.1$

Fig. 5.26 shows the effect of space between the two heat sources on surface temperature. The surface temperature is shown for  $Re = 350$  and  $Ri = 0.1$  with heat source thickness  $H/L = 0.25$  at  $t = 20$ . The first heat source is located at  $x = 2$  to  $3$ . The different locations of the second heat source are  $x = 4$  to  $5$  and  $x = 6$  to  $7$ . From Fig. 5.26, the second heat source surface temperature decreases with the increases of space between heat sources due to increase of boundary layer thickness. There is no change of temperature of the first heat source with increase of space between heat sources.

The Fig. 5.27 also shows the effect of space between two heat sources on surface temperature. The surface temperature is shown for  $Re = 350$  and  $Ri = 0$  with heat source thickness  $H/L = 0.25$  at  $t = 20$ . The different locations of the second heat source are  $x = 4$  to  $5$  and  $6$  to  $7$ . Like Fig. 5.26, the temperature is coming down with increase in the space between the heat sources.

Figs. 5.28 and 5.29 shows the effect of space between two heat sources on vorticity contours for the above case. The vorticity values are more on second heat source as the space decreases between two heat sources due to the wake formation behind the first heat source module. The wake behind the first heat source is alter the flow field on second heat source and increases the vorticity and surface temperature values.

Fig 5.30 shows the result of the effect of the Reynolds Number on the non dimension

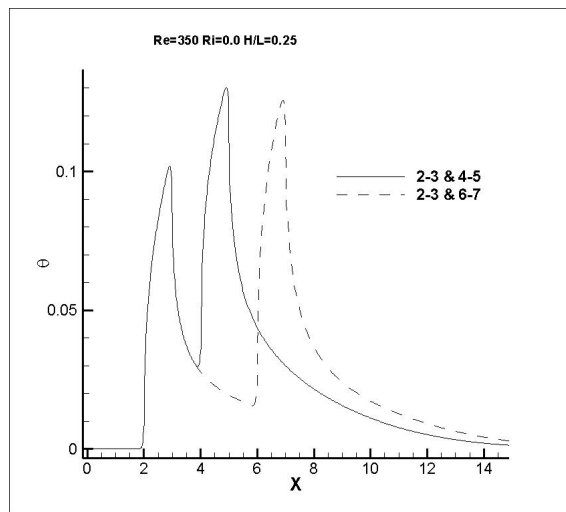


Figure 5.27: Effect of space between heat source module on surface temperature for  $Ri = 0$

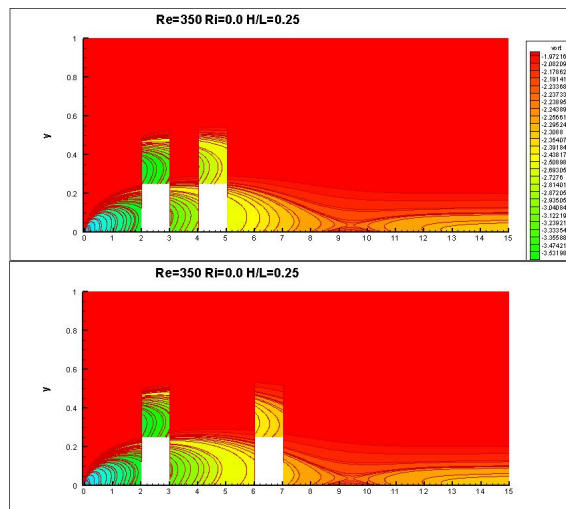


Figure 5.28: Effect of spacing of heat source module on Vorticity contours for  $Ri = 0$

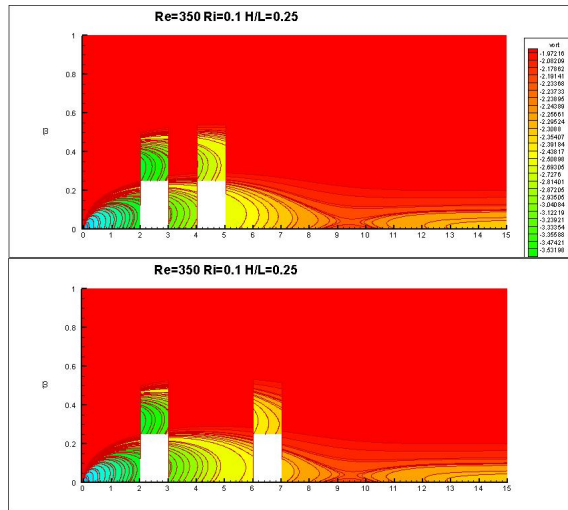


Figure 5.29: Effect of spacing of heat source module on Vorticity contours for  $Ri = 0.1$

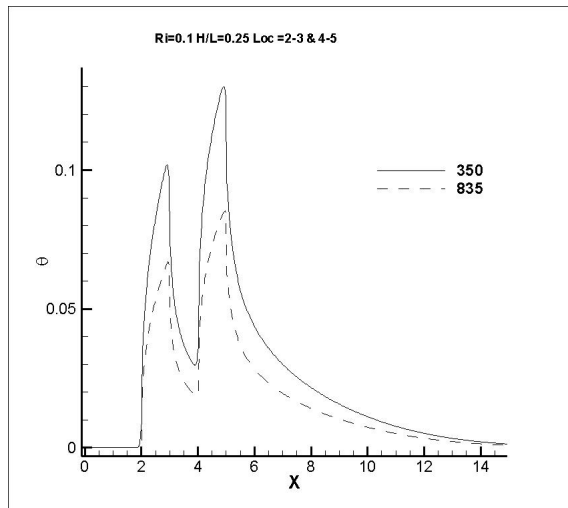


Figure 5.30: Effect of Reynolds Number on surface temperature of the plate

temperature on the flat plate. The plots are for Richardson Number  $Ri = 0.1$ , Flush source thickness  $H/L = 0.25$  with heat source location  $x = 2$  to  $3$  and  $4$  to  $5$ . The cases plotted are  $Re = 350$  and  $835$ . It shows that there is a decrease in the temperature as the Reynolds number is increased. With the increase in the Reynolds Number there is increase in the fluid velocity which increase in the heat dissipation above the plate which lowers the temperature.

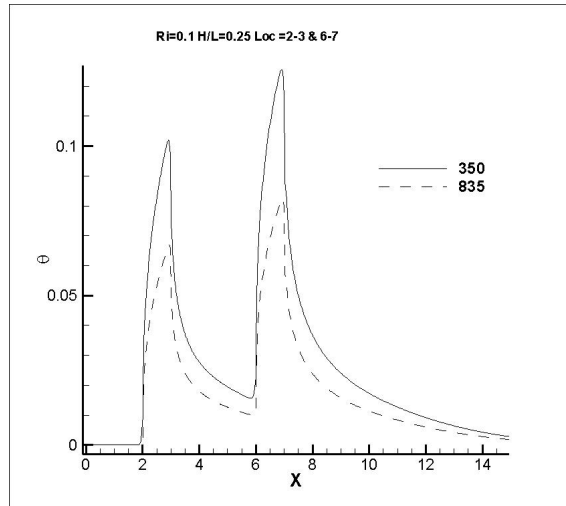


Figure 5.31: Effect of Reynolds Number on surface temperature of the plate

Fig 5.31 also shows the same results for Reynolds Number,  $Re = 350$  and  $835$  with Richardson Number,  $Ri = 0.1$  heat source thickness  $H/L = 0.25$  and heat source location  $2$  to  $3$  and  $6$  to  $7$ .

Fig 5.32 and Fig 5.33 shows the effect of the Reynolds Number on the vorticity pattern in the flow field. Fig. 5.32 gives the difference for  $Re = 350$  and  $835$  with Richardson Number  $Ri = 0.1$ , heat source thickness,  $H/L = 0.5$  with heat source location  $2$  to  $3$  and  $4$  to  $5$ , while Fig. 5.33 shows the difference for Fig. 5.32 gives the difference for  $Re = 350$  and  $835$  with Richardson Number  $Ri = 0.1$ , heat source thickness,  $H/L = 0.5$  with heat source location  $x = 2$  to  $3$  and  $4$  to  $5$  with heat source thickness  $H/L = 0.25$ . It shows that with the increase in the Reynolds Number the vorticity increase on the surface.

The average nusselt number and maximum surface temperature is obtained and shown in the Table.5.2. The average nusselt number is shown for all the surfaces, ie. left, top and right surfaces. From Table. 5.2, one can notice that the nusselt number value is high

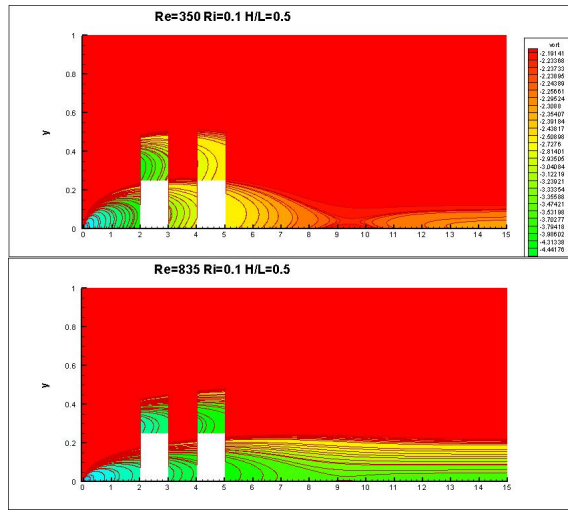


Figure 5.32: Effect of Reynolds Number on vorticity contours in flow field for  $H/L = 0.5$

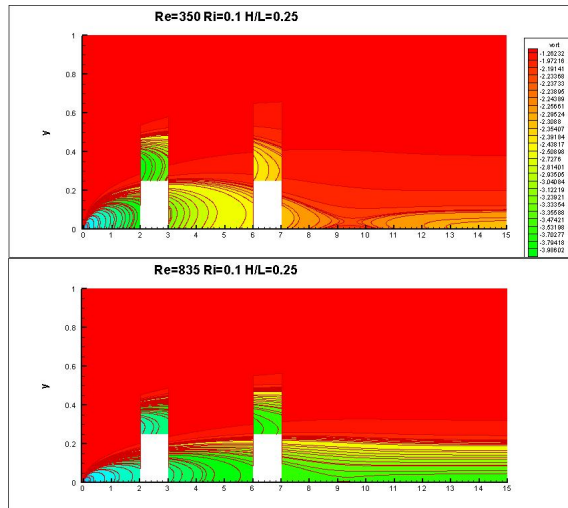


Figure 5.33: Effect of Reynolds Number on vorticity contours in flow field for  $H/L = 0.25$

Table 5.2: Average Nusselt number and maximum surface temperature for the double heat source modules

<i>S.no</i>	Re	Ri	H/L	Loc	Nu(L.F)	Nu(T.F)	Nu(R.F)	$\theta$
1	350	0	0.25	2-3	39.6862	7.0600	5.7140	0.1020
				4-5	11.3887	4.4897	4.4319	0.1301
2	350	0	0.25	2-3	39.6862	7.0600	5.7140	0.1020
				6-7	17.5607	5.0709	4.8015	0.1255
3	350	0	0.50	2-3	29.7646	5.2950	4.2855	0.0765
				6-7	13.1705	3.8032	3.6011	0.0942
4	435	0	0.25	2-3	50.9659	8.0076	6.3369	0.0918
				4-5	13.2954	5.0353	4.9197	0.1171
5	350	0.1	0.25	2-3	39.7270	7.0645	5.7166	0.1019
				4-5	11.3975	4.4993	4.4338	0.1300
6	350	0.1	0.50	2-3	29.7876	5.2975	4.2870	0.0764
				4-5	8.5464	3.3738	3.3250	0.0975
7	835	0.1	0.25	2-3	119.0226	11.9444	8.6802	0.0669
				4-5	20.6682	7.6074	6.7537	0.0852
8	835	0.1	0.25	2-3	119.0203	11.9442	8.6801	0.0669
				6-7	35.0584	8.1568	7.3158	0.0824
9	350	0.1	0.25	4-5	41.3308	6.7715	5.4917	0.1101
				6-7	11.1201	4.3559	4.4249	0.1338
10	350	0.1	0.25	2-3	39.7252	7.0643	5.7165	0.1019
				6-7	17.5724	5.0744	4.8020	0.1255
11	350	0.3	0.25	2-3	39.8083	7.0736	5.7218	0.1018
				4-5	11.4150	4.5066	4.4376	0.1299

for the first heat source compared to second heat source for a given plate. As we have seen in the results of the single heat source module, similarly for a given heat source the average nusselt number value is higher for left surface and lowest for the right surface. The surface temperature of the second heat source is higher than the first heat source due to increase of boundary layer thickness.



# Chapter 6

## Conclusion

Mixed convection flow over of heat source modules mounted on a horizontal plate has been studied numerically and reported here. Present results are valid when the buoyancy force effects are small compared to forced convection effects. The two dimensional incompressible flow with the buoyancy term is modeled using Boussinesq approximation. The governing equations are solved in stream function and vorticity formulation using high accuracy finite difference schemes. Results are reported for flushed heat source modules and heat source modules with thickness. Results are given with different combination of Reynolds and Richardson numbers for flushed heat sources and heat sources with thickness mounted on a horizontal plate. We have taken the Prandtl number ( $Pr$ ) value of air to be 0.7 for all the cases. The average Nusselt number and maximum surface temperature values are given for single and double heat source modules with and without thickness.

From the results the following conclusions:

- The maximum surface temperature on the heat source is decreases with the increase of free stream velocity .
- The maximum surface temperature on the heat source is decreases with the increase of heat input of the heat source.
- The maximum surface temperature on the heat source is increases with increase of distance of the heat source from the leading edge of the plate due to increase of boundary layer thickness.

- The surface temperature of the plate is decreases with the increase of thickness of the heat source module due to increase of surface area.
- The surface temperature of the second heat source is increases with the decrease of distance between the two heat sources.
- The surface temperature is higher on the second heat source compared to first heat source.
- The average Nusselt number values are increases with the increase of free stream velocity and heat input of the heat source.
- The average Nusselt number values are highest and lowest on the left and right faces of the heat sources.

# Bibliography

- [1] A.D.Kraus and A.Bar-Cohen, Thermal Analysis and Control of Electronic Equipment. Hemisphere, New York ,1983.
- [2] B.H. Kang and Y. Jaluria. Natural convection heat transfer characteristic of a protruding thermal source located on a horizontal and vertical surface. International Journal of Heat and Mass Transfer, Vol.33, pp. 1347-1357, 1990.
- [3] M.Fuji, T. Tomimura and X.Zhang. Natural air cooling of an array of IC boards,” Advances in electronic packaging, ASME-EEP, Vol. 10,pp. 823-828, 1995.
- [4] M.Afrid and A.Zebib,’Natural convection cooling of heated components mounted on a vertical wall’ Numerical Heat Transfer, Vol. 15.pp. 243-259, 1989.
- [5] K.A.Park,and A.E.Bergles,”Natural convection heat transfer characteristic of simulated microelectronic chips” ASME Journal of heat transfer, Vol. 109,pp. 90- 96, 1985.
- [6] F.P. Incropera. Convection heat transfer in electronic equipment cooling. ASME Journal of Heat Transfer, Vol. 110, pp. 1097-1109, 1988.
- [7] A.Zebib and Y.K.Wo.”A two dimensional conjugate heat transfer model for forced air cooling of a electronic devices” Proceedings IEEE electronic packaging conference,Orlanado, FL, 1986.
- [8] J.Davalath, and Y.Bayazitoglu, Forced convectioncooling across rectangular blocks. Transactions of ASME Journal of Heat-Transfer, Vol.109, pp.321-327, 1989.

- [9] K.J.Kennedy, and A.Zebib," Combined free and forced convection between horizontal parallel planes;Some case studies ,"International Journal of heat and mass transfer , Vol:26, pp.471-474, 1983.
- [10] B.H.Kang, Y.Jaluria. and S.S.Tewari."Mixed convection transport from an isolated heat source module on a horizontal plate".Transactions of the ASME Journal of Heat Transfer, Vol 112,pp 653661, 1990.
- [11] B.H. Kang, Y. Jaluria, S.S. Tewari, Mixed convection transport from an isolated heat source module on a horizontal plate, J. Heat Transfer,Vol. 112,pp. 653-661, 1990.
- [12] B. Gebhart, R.L. Mahajan, Y. Jaluria and B. Sammakia, Buoyancy Induced Flows and Transport, Taylor and Francis,1988.
- [13] K. Venkatasubbaiah, The effect of buoyancy on the stability mixed convection flow over a horizontal plate, European Journal of Mechanics -B/Fluids, Vol. 30(5), pp-526-533,2011.
- [14] J.D Anderson,"Computational fluid dynamics: The basics with application" Mc Graw Hill Publisher,1985.
- [15] T.K.Sengupta ,"Fundamentals of Computational fluid dynamics: University press, India , 2004.